

**Submission of revised version of the manuscript (2<sup>nd</sup> iteration):**

CPD 11, 5605-5649, 2015:

Regional climate signal vs. local noise: a two-dimensional view of water isotopes in Antarctic firn at Kohnen station, Dronning Maud Land

*Thomas Münch et al.*

Dear Prof Eric Wolff,

along with this document we hand in the second revision of the manuscript entitled above.

In the revision, we have addressed all issues raised by both reviewers. Main focus was given on the diffusion issue raised by reviewer 1. However, his concerns were partly due to some misunderstandings. The point of confusion was whether one asks for the effect of diffusion on a specific frequency band (by passing the time series through a narrow band pass filter), or for the diffusion effect on the complete record analysed at a certain resolution (e.g., decadal). The latter is addressed in our manuscript and, given that our description in the manuscript was ambiguous (talking about time scale but meaning resolution), we have rephrased all relevant parts in the manuscript to make this clear. The second major point is the trend detection experiment where we now account for the effect of diffusion of the annual noise level, which results in slightly more optimistic results.

Please find attached the one-to-one response to the reviewer comments with all detailed changes we made, as well as a marked-up manuscript version created with `latexdiff`.

Kind regards

Thomas Münch

1  
2  
3  
4  
5  
6  
7  
8  
9  
10  
11  
12  
13  
14  
15  
16  
17  
18  
19  
20  
21

## Response to the reviewers

Review of revised version of CPD 11, 5605-5649, 2015: Regional climate signal vs. local noise: a two-dimensional view of water isotopes in Antarctic firn at Kohnen station, Dronning Maud Land

Thomas Münch et al.

13th June 2016

We thank both reviewers for their constructive comments. Please find below our detailed answers. The reviewer comments are typeset in *italics*, our author comments in upright **blue font**.

Anonymous referee #1:

### **1 General Comments on the revised version**

*This revised version of this work presents many improvements compared to the initial submission. I would like to thank and congratulate the authors for delivering a text that reads significantly easier and presents results and conclusions in a much improved way. I think that especially the restructuring of the text was a successful move. The manuscript can be with a little bit more work be ready for acceptance and thus I recommend its publication with minor revisions.*

22 *I have one rather major comment that I would like the authors to look into and*  
23 *consider some small changes in the text and a few minor corrections/ suggestions.*

## 24 **1.1 The influence of diffusion**

25 *With the revised version came a rather extensive consideration on the effects of firn*  
26 *isotope diffusion. This is very welcome; almost necessary though with this extra ma-*  
27 *terial added I was able to spot caveats that need extra consideration in my view. In*  
28 *their answer to the frst review Münch et al suggest that (p3185-90) diffusion works*  
29 *equally on the climatic signal as well as the post depositional noise. Sure enough if*  
30 *you are only focusing on the inter-annual signals diffusion will equally attenuate post*  
31 *depositional noise and anything climatic-driven in these frequency bands. But obvi-*  
32 *ously when you are looking at two meters of core at a place wth accumulation as low*  
33 *as 6 cm/y ice eq. there is more than inter-annual you are looking at. And certainly*  
34 *this is also the case when you are after “warming” trends in the Holocene section*  
35 *of the EDML deep core. You can certainly not expect diffusion to work equally on*  
36 *those bands.*

37 **AC:**

38 **The reviewers comment contains some valid concerns but also some misunderstand-**  
39 **ings.**

40 **1.) Diffusion works equally on the climatic signal as well as the post depositional**  
41 **noise (‘stratigraphic noise’) on all time scales. It only does not affect the noise due**  
42 **to the measurement process (now called  $\sigma_{\text{CRDS}}$  following the notation proposed by**  
43 **the reviewer) which is added after the diffusion has already acted on the signal.**

44 **2.) Of course it is correct that the effect of diffusion depends on frequency (as it is**  
45 **obvious from the exponential dependence on frequency in Eq. (B2) in our appendix**  
46 **B). The point of confusion is whether one asks for the effect of diffusion on a specific**  
47 **frequency band (e.g. decadal variability which would correspond to the signal after**  
48 **passing it through a narrow bandpass filter), or if one asks for the effect of the diffu-**  
49 **sion on the complete record analysed at a certain resolution (e.g. decadal resolved,**  
50 **seasonally resolved). We adress the latter problem because one aim of the discussion**

51 is the variability in the EDML core data from Oerter et al., which is given at decadal  
52 resolution. We understand that the description in the manuscript was ambiguous  
53 (talking about time scale but meaning resolution) and thank the reviewer to pointing  
54 us to this. In our case of decadal resolution, the quantity of interest is the variance  
55 determined on all frequencies from 0 to the fastest frequency resolved by a decadal  
56 resolution (Nyquist frequency). On each frequency in this range, diffusion has a  
57 certain influence on the stratigraphic noise (and the same on any climatic-driven  
58 signal!). If we want to estimate the influence of diffusion at decadal resolution, we  
59 thus have to integrate over the total frequency range ( $0-0.05\text{ yr}^{-1}$ ), as it is done in  
60 Appendix B. We rephrased the manuscript at several points (P2 L14; P13 L25-27;  
61 P14 L1-2,10-11,16,19; P15 L25; P16 L10,17; P19 L7-8; P23 L16; P24 L9-10,23; Table  
62 1+2; Fig. 8), basically replacing “time scale” by “resolution” to clarify that we talk  
63 about the signal at a given resolution and not the effect on a certain frequency band.  
64 3.) The reviewer is right that, in the trend scenario, omitting the diffusion led to  
65 a slightly pessimistic scenario as we used the annual noise variance levels from the  
66 trench data neglecting diffusion. We now present the more realistic case where we  
67 account for the diffusion of the noise (but not for the trend as here the diffusion  
68 effect is negligible). This reduces the noise level by  $\sim 27\%$ , leading to slightly more  
69 optimistic results. The changes are implemented in the manuscript on P17 L28-29  
70 with a reference to Appendix B where we explicitly explain: “The annual noise levels  
71 given in Table 2 are therefore only valid for the uppermost part of the firn column  
72 where diffusion is almost negligible. In the deeper parts of the firn, they have been  
73 affected by diffusion. In our simplified trend detection experiment, we assume over  
74 the first 9 m of firn ( $\sim$  the last 50 years) an average annual layer thickness of 15 cm  
75 and a mean diffusion length of  $\sigma \sim 5$  cm (Johnsen, 2000). Evaluation of Eq. (B3)  
76 then gives an average reduction of the annual noise level to  $\sim 73\%$  of the original  
77 value.” The results of the trend detection experiment have been updated accordingly  
78 (P18 L6-13; P19 L18; Fig. 9).

79

80 **1.1.1 On Appendix B**

81 *Firstly I would like to point out that even though mathematically correct your eq. B2*  
82 *is not what you see in van der Wel et al or any of the other diffusion works that I*  
83 *am aware of. It works much more intuitively that the units of the diffusion length  $\sigma$*   
84 *should be the same as the units of the frequency axis ie expressed in terms of depth*  
85 *or time. I can understand that by introducing the accumulation term  $b$  in there you*  
86 *out things in order but I am also afraid this may create confusion. I will leave it up*  
87 *to the authors to decide what works best.*

88 **AC:**

89 Both formulations are mathematically equivalent and we prefer to directly work in  
90 the time domain here. The translation from one to the other formulation is just the  
91 multiplication with the annual layer thickness and should thus not cause confusion  
92 to the reader. Nevertheless, we have included right after Eq. (B2) the explanation:  
93 “where  $\dot{b}$  is introduced in order to work in the temporal domain, thus with frequency  
94 measured in  $\text{yr}^{-1}$ .”

95

96 *However I think there is an error in your treatment of diffusion in this section*  
97 *and subsequently on the conclusions you draw from this thereafter. Calculating the*  
98 *integral over the 0 to  $f_{nyq}$  band will indeed give you the variance of your signal. But*  
99 *it will give you the total variance or total power of the signal over the full spectrum*  
100 *of frequencies your analytical resolution is able to deliver. As a result, I think you*  
101 *are wrong by saying that the reduction of the annual signal power (you write “annual*  
102 *noise power” but I assume you mean “annual signal power”) is only 0.095 of  $P_0$ .*  
103 *In fact all you are calculating in eq. B3 is the cumulative distribution function of*  
104 *your Gaussian transfer function. And this reflects the loss of power you have because*  
105 *of your non-perfect sampling scheme of  $0.05 \text{ yr}^{-1}$ . If you were able to sample at*  
106 *infinite frequency there will be no loss really.*

107 **AC:**

108 The reviewer points to three related but separate issues.

109 1. that we integrate from 0 to  $f_{nyq}$ . As described in the answer to the second last  
 110 comment, we do this by purpose but now improved the description at the relevant  
 111 parts of the manuscript (see our second last comment) to avoid confusion between  
 112 decadal resolved signal and signal analysed at the decadal frequency band.

113 2. “you write ‘annual noise power’ but I assume you mean ‘annual signal power’”  
 114 – no, we mean annual noise power. Here, we explicitly talk about the reduction  
 115 of the annual stratigraphic noise level by diffusion, not about the effect of diffusion  
 116 on climate signals or any signal in general. The noise can be treated conveniently  
 117 because we can assume it is white, thus a constant in the spectrum, and we can  
 118 therefore solve the integral Eq. (B3) analytically. The power spectrum of a climate  
 119 signal is more complicated (e.q., a power law), and calculating the effect of diffusion  
 120 might be much more complex.

121 3. “this reflects the loss of power you have because of your non-perfect sampling  
 122 scheme of  $0.05 \text{ yr}^{-1}$ . If you were able to sample at infinite frequency there will be  
 123 no loss really”. No, this is not the case. We compare the diffused to the undiffused  
 124 case, starting from annual resolution and assuming thereby that the annual noise  
 125 level inferred from the trench data was not much affected by diffusion already. In the  
 126 undiffused case and for white noise, the power spectrum is a constant  $P_0$ . Then the  
 127 integral over all frequencies from 0 to the decadal Nyquist frequency  $f_0 = 0.05 \text{ yr}^{-1}$   
 128 gives the total noise variance at decadal resolution:

$$129 \quad \text{var}(X)_{10\text{yr}} = 2P_0 \int_0^{0.05\text{yr}^{-1}} df = 0.1 \text{ yr}^{-1} P_0 \quad (1)$$

130

131 This is a common result: When you average an annually resolved time series down  
 132 to decadal resolution, white noise is reduced by a factor of 10.

133 For the diffused case we have to use the result of Eq. (B3):

$$134 \quad \text{var}(X)_{10\text{yr,diff}} = P_0 \sqrt{\pi} / (2\pi\sigma\dot{b}^{-1}) \text{erf}(2\pi\sigma\dot{b}^{-1}f_0) \sim 0.095 \text{ yr}^{-1} P_0. \quad (2)$$

135

136 Comparing the two results gives a relative difference of only 5% as stated in the  
 137 manuscript. To avoid confusion, we added the result of the integral in Eq. (B1) for

138 undiffused white noise (P25 L6-7), and improved the wording when discussing the  
139 result of Eq. (B3) (P25 L15-20).

140

141 *Instead what you probably want to look into is the value of eq. B1 for the various*  
142 *frequencies (depth or time domain). Suppose we are looking at a section close to the*  
143 *firn-ice transition. The annual layer thickness there is about 7 cm ice eq. With a dif-*  
144 *fusion length of 8 cm your diffusion transfer function gives (eq. B1) for  $f = 14.2 \text{ m}^{-1}$*   
145 *roughly  $10^{-6}$ – $10^{-7}$ . Essentially at that depth diffusion has “killed” everything in the*  
146 *range of 5-10 cm. This is roughly anything sub annual, annual and slightly longer*  
147 *than that. In fact decadal signals at this depth have lost 75% of their power.*

148 AC:

149 We thank the reviewer for his calculations. However, the core aim of our manu-  
150 script is to discuss the signal and noise in the trench record and the implications.  
151 Accounting for diffusion is needed to infer about the potential signal and noise in  
152 the Kohnen record and here analysing the effect of diffusion of a record at a certain  
153 resolution (thus integrating across frequencies) is the appropriate metric. Discussing  
154 the effect of diffusion on certain frequency bands, which is an interesting topic by  
155 itself, is beyond the scope of the manuscript.

156

157 *In your analysis you choose a hypothetical value for the  $f_{nyq} = 0.05 \text{ yr}^{-1}$ . This is*  
158 *equivalent to a resolution of 10 years and very roughly a sample resolution of more*  
159 *than 1 meter..! The whole discussion becomes irrelevant if you sample your core at*  
160 *a 1 m resolution. Can you double check this value and redo your calculations with*  
161 *something more relevant? I would say a 0.05 m sampling scheme is something to*  
162 *start with.*

163 AC:

164 The 10 year resolution is relevant for the discussion of the EDML record which is  
165 discussed at a decadal resolution in Oerter et al.

166

167 **1.1.2 On Table 2 and section 4.2 in the manuscript**

168 *In Table 2 and section 4.2 the authors calculate the comparison of measurement*  
169 *noise to the variance of the post depositional noise on various time scales. The Table*  
170 *works very nice as it is (though I would strongly suggest a change in the symbol of the*  
171 *measurement noise – see comment below). Nevertheless I think that it would be very*  
172 *informative to calculate the effect of diffusion on these cycles at the firn-ice transition*  
173 *(where the diffusion process is finished and pore are well closed) as well and presented*  
174 *in the same or a separate table. This will give a more representative picture of how*  
175 *things really look like when one wants to look further deep in the core. In fact I*  
176 *have some of these back of the envelope calculations ready here for the authors. All*  
177 *calculations assume 8 cm diffusion length for  $\delta^{18}\text{O}$  and an accumulation of 7 cm/y*  
178 *ice eq. With  $\mathcal{G}$  I symbolise the value of the Gaussian transfer function.*

179 *Seasonal (I use 0.25 of a year – 0.0175 m - 57.1  $\text{m}^{-1}$ ):  $\mathcal{G} = 10^{-25}$  Diffusion kills*  
180 *all...practically zero of this signal is left. Measurement noise dominates everything*  
181 *in this frequency band.*

182 *Annual case 1 (0.07 m - 14.2  $\text{m}^{-1}$ ):  $\mathcal{G} = 6 \cdot 10^{-6}$ , Practically same as seasonal.*  
183 *Measurement noise dominates again.*

184 *10 yr case 2 (0.7m - 1.42  $\text{m}^{-1}$ ):  $\mathcal{G} = 0.25$ , variance of noise =  $0.75/4 = 0.1875$*   
185 *permile  $\Delta\delta^{18}\text{O} = 0.1875 = 0.48$ . So roughly post depositional and measurement*  
186 *noise contribute equally in this case.*

187 **AC:**

188 **We thank the reviewer for his calculations. However, as described above, this is**  
189 **beyond the aim of the manuscript where we only touch the diffusion topic to be able**  
190 **to discuss the EDML record and the trend detection experiment. As a side note, we**  
191 **don't understand why the transfer function in the figure provided by the reviewer is**  
192 **a straight line whereas the Gaussian in a log-linear figure should reflect a quadratic**  
193 **behaviour. Also, although qualitatively correct, using the Gaussian transfer function**  
194 **for diffusion given in Eq. (B2) we cannot reproduce the numbers the reviewer has**  
195 **calculated for the three exemplary time scales. We can reproduce the graph when**

196 replacing the square term in the exponential by a multiplication with two but we  
197 don't see a physical motivation for such an equation.

198

## 199 **1.2 Specific comments**

200 *I have a few specific comments on the rest of the manuscript:*

201 *P5L1-8: It would be nice for the readers to have a feeling of how much time it took*  
202 *sampling the two trenches. In other words for how long was the snow-firn of the*  
203 *trenches exposed to the air before they were sampled?*

204 **AC:**

205 **At P5 L20-21 we added this information: "The sampling of each trench was com-**  
206 **pleted within 24 h, respectively."**

207

208 *P16L2: I am not sure that adding the term "anthropogenic" is very relevant here.*  
209 *You are investigating the detectability of the isotope signal in resolving a warming*  
210 *trend. This does not necessarily say anything about the origin of the warming trend.*

211 **AC:**

212 **We agree with this and have removed the word "anthropogenic".**

213

214 *P16L8: I do not understand why densification is of importance only for undated*  
215 *samples. Can you elaborate?*

216 **AC:**

217 **Our phrasing was maybe not concise enough here. We have reformulated the sen-**  
218 **tence to (P16 L7-9): "Densification is only of importance when studying the isotopic**  
219 **time series in the depth domain as here, constantly sampled data will contain noise**  
220 **levels on varying time scales."**

221

222 *P16L10: 5% is not a correct estimate. See comments above on Appendix B.*

223 **AC:**

224 At this point we compare the noise level at decadal resolution between the case  
225 without diffusion and the case with diffusion. Thus, the stated percentage means  
226 that in the diffused case the noise level at decadal resolution is (only) reduced by  
227 5% more compared to the undiffused case. We have rephrased this part to make  
228 this clear (P16 L10-11): “[...] at decadal resolution below the firn-ice transition  
229 the noise level at Kohlen station is only 5 % smaller as compared to the undiffused  
230 case (Appendix B and Table 2).” See also our answers to the reviewer comments on  
231 Appendix B.

232

233 *Throughout the text and in Table 2 I would suggest that you change the measurement*  
234 *noise to something like  $\sigma_{CRDS}$  or similar. The symbol  $\Delta$  often refers to an offset or*  
235 *an excess signal or a bias in measurements.*

236 AC:

237 We agree with the reviewer that the symbol  $\Delta$  was not an appropriate choice for the  
238 measurement uncertainty. We have adopted the change suggested by the reviewer  
239 (P16 L18 and Table 2).

240

241 **Anonymous referee #2:**

242 *After revisions, this work is greatly improved, and of direct relevance to the broader*  
243 *ice core community. The paper significantly improves our understanding of extract-*  
244 *ing ice core climate signals in low accumulation areas, as well as how to think about*  
245 *climate signals in already drilled ice cores.*

246 *Suggested edits, but not required:*

247 *pg 4 line 3-16, It would be useful to the reader to include the mean accumulation*  
248 *rate with each of the studies listed. for example, a lack of correlation at decadal time*  
249 *scales cannot be put into context without accumulation rate.*

250 AC:

251 We agree that this is useful and have cited some respective accumulation values (not  
252 all in order to maintain the text flow) from the literature (P4 L3-20).

253

254 *pg 4, line 5-7, It would be useful to the reader to place the F-value in context. What*  
255 *does this number mean to the reader? How could this compare, for example, to a*  
256 *higher accumulation region? Placing context on this value would be beneficial in*  
257 *later section of the paper when this is discussed.*

258 AC:

259 To provide more context for the reader we complemented the sentence in P4 L8  
260 by “[...], implying that the climate signal content of a single core is much smaller  
261 than the noise level (14 and 4 %, respectively)”. A comparison to high-accumulation  
262 regions on Greenland is now included citing Fisher (1985) who estimated SNRs for  
263 Greenland ice cores of  $F > 1$  (P4 L18-20).

264

265 *pg 4 line 23, it would be useful to clarify what you mean by low accumulation region.*  
266 *although you state earlier that this broadly means less than 10cm per year, I think*  
267 *the mean value deserves mentioning for comparison to the studies listed in the para-*  
268 *graphs above.*

269 AC:

270 We now have mentioned the local accumulation rate at the study site (64 mm  
271 w.eq./yr) here (P4 L27).

272

273 *pg 9 line 12-14, interesting that this may be seasonality!*

274 AC:

275 Yes, indeed.

276

277 *pg 12 line 4-5, this sentence nicely sets up your discussion points.*

278 AC:

279 Thank you.

280

281 *pg 13 line 14-23, well-written and provides good context.*

282 AC:

283 Thank you.

284

285 *pg 17 line 24 + pg 19 line 14, I suggest to use just “model” or some other option*  
286 *rather than “toy model”.*

287 **AC:**

288 **We have changed the phrasing at these two points to “simplified model experiment”.**

289

Manuscript prepared for Clim. Past Discuss.

with version 2015/04/24 7.83 Copernicus papers of the  $\LaTeX$  class copernicus.cls.

Date: 13 June 2016

# **Regional climate signal vs. local noise: a two-dimensional view of water isotopes in Antarctic firn at Kohnen station, Dronning Maud Land**

**Thomas Münch<sup>1,2</sup>, Sepp Kipfstuhl<sup>3</sup>, Johannes Freitag<sup>3</sup>, Hanno Meyer<sup>1</sup>, and  
Thomas Laepple<sup>1</sup>**

<sup>1</sup>Alfred Wegener Institute Helmholtz Centre for Polar and Marine Research, Telegrafenberg A43, 14473 Potsdam, Germany

<sup>2</sup>Institute of Physics and Astronomy, University of Potsdam, Karl-Liebknecht-Str. 24/25, 14476 Potsdam, Germany

<sup>3</sup>Alfred Wegener Institute Helmholtz Centre for Polar and Marine Research, Am Alten Hafen 26, 27568 Bremerhaven, Germany

Correspondence to: T. Münch (tmuench@awi.de)

## Abstract

In low-accumulation regions, the reliability of  $\delta^{18}\text{O}$ -derived temperature signals from ice cores within the Holocene is unclear, primarily due to the small climate changes relative to the intrinsic noise of the isotopic signal. In order to learn about the representativity of single ice cores and to optimise future ice-core-based climate reconstructions, we studied the stable-water isotope composition of firn at Kohnen station, Dronning Maud Land, Antarctica. Analysing  $\delta^{18}\text{O}$  in two 50 m long snow trenches allowed us to create an unprecedented, two-dimensional image characterising the isotopic variations from the centimetre to the hundred-metre scale. Our results show seasonal layering of the isotopic composition but also high horizontal isotopic variability caused by local stratigraphic noise. Based on the horizontal and vertical structure of the isotopic variations, we derive a statistical noise model which successfully explains the trench data. The model further allows to determine an upper bound for the reliability of climate reconstructions conducted in our study region ~~on seasonal to inter-annual time scales~~ at seasonal to annual resolution, depending on the number and the spacing of the cores taken.

## 1 Introduction

Ice cores obtained from continental ice sheets and glaciers are a key climate archive. They store information on past changes in temperature in the form of stable water isotopes (EPICA community members, 2006), in greenhouse gas concentrations via trapped air (Raynaud et al., 1993) and in many other parameters such as accumulation rates (e.g., Mosley-Thompson et al., 2001) or aerosols (e.g., Legrand and Mayewski, 1997). Analysis of the isotope ratios recorded in single deep ice cores provided milestones in the palaeoclimate research, including the investigation of glacial-interglacial climate changes (Petit et al., 1999) and the existence of rapid climate variations within glacial periods (Dansgaard et al., 1993).

In contrast to the coherent view established from polar ice cores for millennial and longer time scales, the reliability of single ice cores as archives of the Holocene climate evolution is less clear (Kobashi et al., 2011). The small amplitude of changes and the aim to reconstruct climate parameters at high temporal resolution poses a challenge to the interpretation of ice-core signals. This is especially true for low-accumulation sites; defined here for accumulation rates below  $100\text{ mm w.eq. yr}^{-1}$  which holds for large parts of the East Antarctic Plateau. There, the non-climate noise – that part of the isotopic record which cannot be interpreted in terms of temperature variations on regional or larger scales; hence including any meteorological, pre- and post-depositional effects that additionally influence the isotopic composition – may often be too high to accurately extract a climatic temperature signal (Fisher et al., 1985). Despite the challenges, quantifying the Holocene polar climate variability is the key foundation to determine the range of possible future climate changes (e.g., Huntingford et al., 2013, and references therein) as well as to test the ability of climate models in simulating natural climate variability (Laepfle and Huybers, 2014).

The quantitative estimation of climate variability from proxy data therefore requires an understanding of the non-climate noise in order to separate them from the climate signal (e.g., Laepfle and Huybers, 2013). Several mechanisms influence the isotopic composition of snow prior to and after its deposition onto the ice sheet. On larger spatial scales, non-climate variability may be introduced by different moisture pathways and source regions (e.g., Jones et al., 2014) as well as spatial and temporal precipitation intermittency (Persson et al., 2011; Sime et al., 2009, 2011; Laepfle et al., 2011). Irregular deposition caused by wind and surface roughness along with spatial redistribution and erosion of snow is a major contribution to non-climate variance on smaller spatial scales (“stratigraphic noise”, Fisher et al., 1985). Wind scouring can additionally remove entire seasons from the isotopic record (Fisher et al., 1983). Vapour exchange with the atmosphere by sublimation-condensation processes (Steen-Larsen et al., 2014) can influence the isotopic composition of the surface layers; diffusion of vapour into or out of the firn driven by forced ventilation (Waddington et al., 2002; Neumann and Waddington, 2004; Town et al., 2008) may represent an additional component of post-depositional change. Finally, diffusion of water vapour through

the porous firn smoothes isotopic variations from seasonal to inter-annual or longer time scales, depending on the accumulation rate (Johnsen, 1977; Whillans and Grootes, 1985; Cuffey and Steig, 1998; Johnsen et al., 2000).

In the last two decades, a number of studies analysed the representativity of single ice cores in recording sub-millennial climate changes. One well-studied region is [the low-accumulation \(38–89 mm w.eq. yr<sup>-1</sup>, Oerter et al., 2000 \)](#) Dronning Maud Land (DML) on the East Antarctic Plateau. Here, Graf et al. (2002) found low signal-to-noise variance ratios ( $F$ ) in 200 year long firn-core records for oxygen isotopes ( $F = 0.14$ ) and accumulation rates ( $F = 0.04$ ); [implying that the climate signal content of a single core is much smaller than the noise level \(14 and 4%, respectively\)](#). On a similar time scale, Karlöf et al. (2006) detected no relationship in electrical properties apart from volcanic imprints between firn cores. Similarly, high-resolution records of chemical trace species from three shallow ice cores [\(Sommer et al., 2000a, b\)](#) [\(Sommer et al., 2000a, b\)](#) showed a lack of inter-site correlation on decadal time scales. These results were supported by process studies comparing observed and simulated snow-pit isotope data (Helsen et al., 2006). Whereas the model-data comparison was successful for coastal high-accumulation regions of DML [\(400 mm w.eq. yr<sup>-1</sup>\)](#), it largely failed on the dryer East Antarctic Plateau [\(70 mm w.eq. yr<sup>-1</sup>\)](#). This dependency between accumulation rate and signal-to-noise ratio was further demonstrated in studies across the Antarctic continent (Hoshina et al., 2014; Jones et al., 2014; McMorrow et al., 2002). [From high-accumulation \(140–520 mm w.eq. yr<sup>-1</sup>\) Greenland ice cores, Fisher et al. \(1985\) estimated signal-to-noise ratios clearly larger than one.](#)

Despite this large body of literature, quantitative information about the signal-to-noise ratios and the noise itself is mainly limited to correlation statistics of nearby cores. While a relatively good understanding of stratigraphic noise exists in Arctic records (Fisher et al., 1985), this does not apply to low-accumulation regions of Antarctica where the accumulated snow is considerably reworked in and between storms (Fisher et al., 1985).

Here we provide a direct visualisation and analysis of the signal and noise in an East Antarctic low-accumulation region [\(64 mm w.eq. yr<sup>-1</sup>\)](#) by an extensive two-dimensional sampling of the firn column in two 50 m long snow trenches. Our approach, for the first

time, offers a detailed quantitative analysis of the spatial structure of isotope variability on a centimetre to hundred-metre scale. This is a first step towards a signal and noise model to enable quantitative reconstructions of the climate signal and their uncertainties from ice cores.

## 5 2 Data and methods

Near Kohlen station ~~on~~in the interior of Dronning Maud Land, close to the EPICA deep ice core drilling site (EDML,  $-75.0^{\circ}$  S,  $0.1^{\circ}$  E, altitude 2892 m a.s.l., mean annual temperature  $-44.5^{\circ}$  C, mean annual accumulation rate  $64 \text{ mm w.eq. yr}^{-1}$ , EPICA community members, 2006), two 1.2 m deep and approximately 45 m long trenches in the firn, named T1 and T2, were excavated during the austral-summer field season 2012/2013 using a snow blower. Each trench was aligned perpendicularly to the local snow-dune direction. The horizontal distance between the starting points of T1 and T2 was 415 m.

An absolute height reference was established using bamboo poles by adjusting their heights above ground with a spirit level. A control measurement with a laser level yielded in each snow trench a vertical accuracy better than 2 cm. No absolute height reference between the two trenches could be established, but, based on a stacked laser level measurement, the vertical difference between the trenches was estimated to be less than 20 cm.

Both trenches were sampled for stable-water-isotope analysis with a vertical resolution of 3 cm. In T1, 38 profiles were taken at variable horizontal spacings between 0.1 and  $\sim 2.5$  m. In T2, due to time constraints during the field campaign, only four profiles at positions of 0.3, 10, 30 and 40 m from the trench starting point were ~~sampled-~~realised. The sampling of each trench was completed within 24 h, respectively. All firn samples ( $N = 1507$ ) were stored in plastic bags and transported to Germany in frozen state. Stable isotope ratios were analysed using Cavity Ring-Down Spectrometers (L2120i and L2130i, Picarro Inc.) in the isotope laboratories of the Alfred Wegener Institute (AWI) in Potsdam and Bremerhaven.

The isotope ratios are reported in the usual delta notation in per mil (‰) as

$$\delta = \left( \frac{R_{\text{sample}}}{R_{\text{reference}}} - 1 \right) \times 10^3, \quad (1)$$

where  $R_{\text{sample}}$  is the isotopic ratio of the sample ( $^{18}\text{O}/^{16}\text{O}$ ) and  $R_{\text{reference}}$  that of a reference. The isotopic ratios are calibrated with a linear three-point regression analysis using in-house standards at the beginning of each measurement sequence, where each standard has been calibrated to the international V-SMOW/SLAP scale. Additionally, a linear drift-correction scheme and a memory-correction scheme (adapted from van Geldern and Barth, 2012) is applied, using three repeated measurements per sample. The analytical precision of the calibrated and corrected  $\delta^{18}\text{O}$  measurements is assessed by evaluating standards in the middle of each measurement sequence. This yields a mean combined measurement uncertainty of 0.09‰ (RMSD).

For the analysis of the measurements, we set up two coordinate systems for each trench (Fig. 1). Surface coordinates refer to a local, curvilinear system with **horizontal axis tangential to the horizontal axis along** the surface height profile and **the** vertical axis denoting the firn depth below the local surface. Absolute coordinates adopt the mean surface height as a reference for a straight horizontal axis, completed by an absolute depth scale.

### 3 Results

#### 3.1 Trench isotope records

The firn samples obtained from trench T1 provide a two-dimensional image of the  $\delta^{18}\text{O}$  structure of the upper  $\sim 1$  m of firn on a horizontal scale of  $\sim 50$  m (Fig. 2a).

The surface height profile of the trench reflects the typical snow topography of the sampling region characterised by small-scale dunes with their main ridges elongated parallel to the mean wind direction (Birnbaum et al., 2010). Trench T1 features one prominent dune located between 25–40 m, accompanied by a dune valley between  $\sim 8$ –18 m, and some

smaller-scale height variations. The peak-to-peak amplitude of the large dune undulation is  $\sim 10$  cm, the entire height variations exhibit a standard deviation (SD) of 2.9 cm.

Overall, the trench  $\delta^{18}\text{O}$  record shows a diverse picture. The delta values in T1 (Fig. 2a) span a range from  $-54$  to  $-34\text{‰}$  with a mean of  $-44.4\text{‰}$  (SD 3.1‰). A similar range of  $-50$  to  $-38\text{‰}$  is observed in T2 (Fig. 3) with a mean of  $-44.0\text{‰}$  (SD 2.7‰). We can identify eight to ten alternating layers of enriched and depleted isotopic composition in the T1 record. The uppermost layer (first 6 cm relative to the surface) essentially shows enriched (mean of  $-42.7\text{‰}$ ) but also strongly variable  $\delta^{18}\text{O}$  values between  $-54$  and  $-34\text{‰}$  (SD 4.4‰), thus already covering the range of the entire trench record. **Less enriched values tend to be located** Stronger enrichment tends to be found in the valleys, however, the limited data do not allow to conclude whether this is a general feature. In an absolute depth of 5–20 cm, a band of generally more depleted  $\delta^{18}\text{O}$  values is found exhibiting less horizontal variability compared to the first layer with a range of  $-54$  to  $-45\text{‰}$  (mean  $-48.5\text{‰}$ , SD 1.9‰). The layering appears strongly perturbed in the depth of  $\sim 60$ –100 cm for profile positions  $< 30$  m. Here, a broad and diffuse region of rather constant  $\delta^{18}\text{O}$  values around  $-40\text{‰}$  is observed, together with a prominent, 20 cm-thick feature of high delta values between 18 and 28 m.

The four  $\delta^{18}\text{O}$  profiles obtained from trench T2 (Fig. 3) show similar features as trench T1. We can identify roughly five cycles in each profile. However, the profiles diverge considerably at depths of 50–90 cm which coincides with the region of strong perturbations identified in T1.

To further analyse the isotopic layering, we determine the pronounced local maxima and minima of each T1  $\delta^{18}\text{O}$  profile and visually assign summer and winter to the depths of these extrema. This results in consecutive horizontal curves tracing the vertical positions of seasonal extrema along the trench (seasonal layer profiles, Fig. 2b). Assuming that respective isotopic extrema occur at the same point in time (summer/winter), the seasonal layer profiles reflect the surface height profile for a given season. However, considering the highly variable isotopic composition observed at the current trench surface (Fig. 2a), this is a rough approximation and the seasonal layer profiles will likely overestimate the past

surface height profiles. Nevertheless, the vertical undulations of the layer profiles show peak-to-peak amplitudes of 6–24 cm (average SD 3.7 cm), comparable to the present surface undulations, and the layers are vertically separated by approximately 20 cm, in accord with the local mean annual accumulation rate of snow ( $64 \text{ mm w.eq. yr}^{-1}$ ) and the mean firn density of  $\rho_{\text{firn}} = 340 \text{ kg m}^{-3}$  measured in trench T1 ( $\rho_{\text{firn}} = 340 \text{ kg m}^{-3}$ ). To study the similarity between the seasonal layer profiles and the present surface height profile, we calculate the standard deviation of their height differences ( $\text{SD}_{\text{surface}}$ ; hence, the SD of each layer profile on surface coordinates). This is compared to the standard deviation of the layer profiles on absolute coordinates ( $\text{SD}_{\text{horiz}}$ ). We find that the first layer profile closely follows the present surface ( $\text{SD}_{\text{horiz}} - \text{SD}_{\text{surface}} = 1.8 \text{ cm}$ ). For the second layer profile, the link with the surface is weaker ( $\text{SD}_{\text{horiz}} - \text{SD}_{\text{surface}} = 1.5 \text{ cm}$ ), and the layer profiles below 20 cm are on average horizontally aligned ( $\text{SD}_{\text{horiz}} - \text{SD}_{\text{surface}} = -0.6 \text{ cm}$ ). This can be explained by an annual reorganisation of the stratigraphy so that aligning the isotopic variations on absolute coordinates is on average more appropriate than the alignment according to a specific surface height profile. The positive autocorrelation with a decorrelation length of  $\sim 6 \text{ cm}$  that is found from the vertical T1  $\delta^{18}\text{O}$  variations after subtraction of the mean trench profile is consistent with this hypothesis.

Due to the on average horizontal stratigraphy of the isotopic composition in the larger part of the trench record all further plots and calculations will be evaluated on absolute coordinates.

### 3.2 Single-profile representativity

The isotope record of trench T1 (Fig. 2a) allows to quantify the horizontal isotopic variability of the snow and firn column in our study region. We observe considerable horizontal variability with a mean variance of  $\sigma_{h,T1}^2 \simeq 5.9 (\%)^2$ , directly affecting the representativity of single trench profiles. To mimic the potential result obtained from correlating two snow pits taken at a distance of 500 m, similarly done in many firn-core studies (e.g., McMorrow et al., 2002), we calculate the pairwise Pearson correlation coefficient between single profiles of T1 and single profiles of T2. We account for potential surface undulations between

the trenches by allowing bin-wise vertical shifts of  $\pm 12$  cm between the T1 and T2 profiles to maximise their correlation. The estimated correlations (Fig. 4) are substantially scattered around a mean correlation of  $\sim 0.50$  ( $SD = 0.13$ ). The relative majority ( $\sim 43\%$ ) of all possible profile pairs ( $N = 152$ ) shows a maximum correlation at a shift of  $+3$  cm which is well below the estimated upper vertical height difference of the trenches.

### 3.3 Mean trench profiles

Spatial averaging is expected to improve the correlation between the trenches compared to the single profiles. We therefore correlate the mean trench profiles of T1 and T2, allowing again for bin-wise vertical shifts of the T2 profile to maximise the correlation.

The mean trench profiles (Fig. 5) are highly correlated ( $r_{T1,T2} = 0.81$  for an optimal shift of  $+3$  cm;  $p = 0.01$ , accounting for the full autocorrelation structure and allowing for vertical shifting), indicating a common isotopic signal reproducible over a spatial scale of at least 500 m. It is interesting to note that this value is above most of the single inter-trench correlations (Fig. 4).

In both mean profiles, we observe five seasonal cycles spanning a range of  $\sim 6$ – $7\%$  at the surface, but being attenuated further down and exhibiting no clear sinusoidal shape in the depth range of 65–90 cm. Interestingly, this obscured part without clearly depleted  $\delta^{18}\text{O}$  “winter” values is found in both trenches, indicating that this feature persists over at least 500 m and is thus likely of climatic origin, e.g., a winter with unusually low precipitation. Despite the statistically significant correlation, pronounced differences between the mean profiles are present, such as a significantly more depleted, respectively more enriched, isotopic composition of the T2 mean between 50–80 cm.

To analyse annual-mean  $\delta^{18}\text{O}$  time series we use different binning methods to average the seasonal trench data with bins defined by (1) the six local maxima determined from the average of the two mean trench profiles, (2) the five local minima, (3) the midpoints of the ascending slopes flanking the maxima and (4) the midpoints of the descending slopes. To display the data on an absolute time axis we assign the year 2012 to the first annual bin. The annual-mean time series derived from the four possible binning sets are averaged to

obtain a single time series for each trench (Fig. 5). The correlation of the average annual-mean  $\delta^{18}\text{O}$  time series of  $r_{\overline{T1}, \overline{T2}} = 0.87_{-0.20}^{+0.07}$  (range represents the four binning methods) is comparable to that of the mean seasonal profiles (0.81). However, five observations of annual means are too short to reliably estimate the correlation and its significance.

### 5 3.4 Spatial correlation structure

We have shown that spatial averaging significantly increases the correlation between the trenches. To learn more about the spatial correlation structure of the trench isotope record, we investigate (1) the inter-profile correlation as a function of profile spacing for T1 and (2) the inter-trench correlation between different sets of mean profiles from T1 and the mean T2 profile.

The inter-profile correlation is estimated as the mean of the correlations obtained from all possible T1 profile pairs separated by a given spacing, allowing a tolerance in the horizontal position of 5%. For the inter-trench correlation, we define a T1 profile stack as the spatial average across a certain number of T1 profiles separated by a given distance, and determine all possible equivalent stacks. The inter-trench correlation with the mean T2 profile is then recorded as the mean across the correlations between the mean T2 profile and all possible T1 stacks.

The inter-profile correlation approaches one for nearest neighbours and rapidly drops with increasing inter-profile spacing before it stabilises around a value of  $\sim 0.5$  for spacings  $\gtrsim 10$  m (Fig. 6). For the inter-trench correlation, we find a steady increase in the correlation with the T2 reference with increasing number of profiles used in the T1 stacks (Fig. 7). Additionally, the correlation increases with a wider spacing between the individual profiles of a stack.

The observed decrease of the inter-profile correlation with distance suggests a horizontal autocorrelation of the isotopic composition. Indeed, a positive autocorrelation of the horizontal  $\delta^{18}\text{O}$  variations of T1 with a decorrelation length of  $\lambda \simeq 1.5$  m is found by applying a Gaussian kernel correlation (Rehfeld et al., 2011) which accounts for the irregular horizon-

tal sampling. As we do not expect any climate-related part of the isotopic record to vary on such small spatial scales, we attribute the observed autocorrelation to noise features.

### 3.5 Statistical noise model

The inter-profile correlation  $r_{XY}$  provides an estimate of the signal-to-noise variance ratio  $F$  of single profiles (Fisher et al., 1985),

$$F = r_{XY} / (1 - r_{XY}). \quad (2)$$

Neglecting the small-scale correlation, we estimate  $F$  from the data using the mean inter-profile correlation for the profile spacings between 10–35 m and find  $F = 0.9 \pm 0.1$ .

Based on our findings, we develop a simple statistical model: We assume that each trench profile consists of the sum of a common climate signal  $S$  and a noise component  $w$  independent of the signal. The noise component is modelled as a first-order autoregressive process (AR(1)) in the horizontal direction. Then, the inter-profile correlation coefficient between profiles  $X$  and  $Y$  becomes a function of their spacing  $d$  (see Appendix A),

$$r_{XY} = \frac{1}{1 + F^{-1}} \left\{ 1 + F^{-1} \exp\left(-\frac{d}{\lambda}\right) \right\}. \quad (3)$$

Here,  $F^{-1} = \text{var}(w) / \text{var}(S)$  is the inverse of the signal-to-noise variance ratio. Using our estimate for  $F$  and the value for  $\lambda$  obtained in the previous section, the model reproduces the observed inter-profile correlations (Fig. 6). Applying the same parameter values, the theoretical inter-trench correlation (Eq. A15) is also in good agreement with the empirical results (Fig. 7). This validates the model and the parameter values ( $F$ ,  $\lambda$ ) from the intra-trench ( $\sim 10$  m) to the inter-trench spatial scale ( $\sim 500$  m).

## 4 Discussion

Our trench data confirm earlier results that individual  $\delta^{18}\text{O}$  firn-core records from low-accumulation regions are strongly influenced by local noise (Fisher et al., 1985; Karlöf et al.,

2006). Going beyond this finding, our two-dimensional  $\delta^{18}\text{O}$  data set also allows to determine the spatial structure and to learn about the causes of the noise. In this section, we discuss our findings in the context of the possible noise sources and derive implications for seasonal to inter-annual climate reconstructions based on firn cores.

#### 5 4.1 Local stratigraphic noise and regional climate signal

A horizontally stratified trench without horizontal isotopic variations would yield perfectly correlated single profiles. Opposed to that, our records show a significant variability in horizontal direction with mean variances ( $\sigma_{h,T1}^2 \simeq 5.9(\text{‰})^2$ ,  $\sigma_{h,T2}^2 \simeq 5.3(\text{‰})^2$ ) that are smaller but of the same order of magnitude as the mean down-core variances ( $\sigma_{v,T1}^2 \simeq 9.5(\text{‰})^2$ ,  $\sigma_{v,T2}^2 \simeq 7.3(\text{‰})^2$ ). In consequence, coherent isotopic features between single profiles separated by the trench distance are only found by chance (Fig. 4: the median correlation is 0.49, only for two pairs ( $\sim 1.3\%$ ) the correlation is  $> 0.8$ ). Thus, single firn profiles from our study region are no representative recorders of climatic isotope signals on the vertical scales analysed here.

On the horizontal scale of the trenches ( $\sim 10\text{--}500\text{ m}$ ), we expect that stratigraphic noise dominates the isotopic variations (Fisher et al., 1985). The observed length scale of the horizontal decorrelation of the noise ( $\lambda \sim 1.5\text{ m}$ ) is similar in magnitude as that on which the local small-scale surface height variations occur, indicating that stratigraphic noise is in fact the prominent noise component in our data.

Despite the low single-profile representativity, the trench record contains a climate signal becoming apparent through the inter-profile correlation of  $\sim 0.5$  remaining on scales on which the stratigraphic noise is decorrelated ( $\gtrsim 10\text{ m}$ ). It appears to be regionally ( $\lesssim 1\text{ km}$ ) coherent as suggested firstly by the comparable values of the inter-profile correlation for spacings  $\gtrsim 10\text{ m}$  and the mean correlation between single T1–T2 records (Fig. 4), and secondly by the common seasonal signal observed in the mean trench profiles (Fig. 5).

Noise is always reduced by averaging profiles; here, the autocorrelation causes nearby profiles to share more common noise variance than profiles at a larger spacing. Therefore, albeit the same number of profiles is averaged, stacks using a larger profile spacing will

exhibit less common noise variance and hence a larger proportion of the underlying signal (Fig. 7). Our results show a minimum profile spacing of  $\sim 10$  m to be optimal.

## 4.2 Representativity of isotope signals on seasonal to inter-annual time scales

For quantitative climate reconstructions from proxy data, a robust estimate of the climate signal is necessary. Based on our statistical noise model, we can estimate the isotopic climate signal content of a profile stack for our study region depending on the number of averaged profiles and their spacing.

To this end, we define the climate representativity of a trench profile stack as the correlation between the stack and a common climate signal (Eq. A14). This signal is identified with the coherent isotope signal of the trench records. A physical interpretation of the climate representativity is then the upper bound of the correlation with a local temperature record, for example from a weather station. However, bearing in mind other influences such as meteorology (variable storm tracks, changing moisture source regions, precipitation-weighting), the true correlation will be lower. In the limit of independent noise our definition of climate representativity is equivalent to the expression derived by Wigley et al. (1984).

In general, climate signals are time-scale dependent. For example, the seasonal amplitude of the isotopic signal is much larger than any variations between the years. On the other hand, one expects larger changes of the climate signal on longer time scales, such as glacial-interglacial cycles. Moreover, not only the climate signal but also the noise can be a function of the time scale. One extreme example for this are the non-climate oscillations of the isotopic composition on up to centennial time scales which have been indicated by snow-pit studies around Vostok station and linked to the movement of accumulation waves on various scales (Ekaykin et al., 2002). Since the climate representativity (Eq. A14) depends on the ratio  $F$  of signal and noise variance, it is in consequence also a function of the time scale.

Here, we assess the climate representativity of firn isotope profiles from our study region for two specific time scales, (1) the original (~~seasonal~~) resolution of the trench data and

(2) an ~~inter-annual time scale~~ annual resolution based on binning the trench data to ~~annual resolution~~.

Analysing ~~seasonal variability~~ the original data, which is dominated by variations on seasonal time scales, the climate representativity can be readily calculated with the model parameters obtained in Sect. 3.5. For the ~~inter-annual time scale~~ analysis at annual resolution, estimates of both annual signal and noise variance are necessary to assess the variance ratio  $F$ . However, the shortness of our trench data ~~on this time scale~~ only allows heuristic estimates (see Appendix A for details). Specifically, for the annual noise variance we discuss two limiting cases: For case I) we assume that the vertical noise is white (best-case scenario), for case II) that the vertical noise shows complete inter-dependence on the sub-annual time scale (worst case). The inverse of the annual signal-to-noise variance ratio,  $F_{\text{annual}}^{-1} = \text{var}(w)_{\text{annual}} / \text{var}(S)_{\text{annual}}$ , used in the model is then  $\sim 1.2$  for case I and  $\sim 8.7$  for case II. A summary of the noise levels is given in Table 2.

For single profiles, the ~~estimated climate representativity on the seasonal time scale~~ climate representativity estimated at seasonal resolution is 0.69 (Fig. 8). ~~On the inter-annual time scale~~ At annual resolution, single profiles show a representativity of 0.67 in the best-case scenario (Fig. 8a) and of 0.32 in the worst-case scenario (Fig. 8b).

Similar to the correlation between the trenches (Fig. 7), the representativity increases with the number of profiles averaged with a stronger increase for larger inter-profile spacings. However, spacings above 10 m do not yield a further increase as the stratigraphic noise is largely decorrelated. To obtain a climate representativity of 0.8 ~~for inter-annual signals at annual resolution~~ with profiles separated by 10 m, a minimum of 3–16 cores ~~is are~~ needed (from best to worst case). Demanding a representativity of 0.9, the number of cores required increases to 6–37.

The modelled single-profile climate representativity ~~for the inter-annual time scale at annual resolution~~ appears consistent with previous findings from Dronning Maud Land. Graf et al. (2002) estimated a low signal-to-noise variance ratio of  $F = 0.14$  obtained from the cross-correlations of 16 annually resolved  $\delta^{18}\text{O}$  records from an area of  $500\text{km} \times 200\text{km}$ . Due to the large inter-core spacings, the stratigraphic noise in the records is decorre-

lated and the variance ratio  $F$  can be translated into a single-profile representativity of  $r_{SX} = 1/\sqrt{1+F^{-1}} \simeq 0.35$ , consistent with our findings for the worst-case scenario. However, the records analysed in Graf et al. (2002) are also subject to dating uncertainties, additional variability caused by spatially varying precipitation-weighting and other effects. Therefore, the similar representativities are not necessarily caused by the high stratigraphic noise level assumed in the worst-case scenario. In addition, our trench data indicate vertical autocorrelation of the noise (Fig. 2b and Sect. 3.1). Thus, the true climate representativity for our study region will likely be in between of our limiting estimates.

Stratigraphic noise does not only affect isotopes but also other parameters measured in ice cores, such as aerosol-derived chemical constituents. Gfeller et al. (2014) investigated the seasonal to inter-annual representativity of ion records from five Greenland firn cores taken at varying distances from 7–10 m in the vicinity of the NEEM drilling site. Using the definition of representativity based on Wigley et al. (1984), they found inter-annual representativities of  $\sim 0.55$ – $0.95$ , depending on the number of averaged cores and the ion species considered. These numbers are slightly higher than our best-case-scenario results for  $\delta^{18}\text{O}$ , which is expected since the accumulation rate at the NEEM site is about three times higher than at Kohnen station (NEEM community members, 2013).

Our estimates for the climate representativity of firn cores hold as long as the signal-to-noise variance ratio  $F$  does not change. Variance-affecting processes such as diffusion and densification have equal influence on signal and noise and thus do not alter the ratio  $F$ . On the other hand, only one component might change over time; e.g., the noise variance might vary due to changing environmental conditions, or the variability of the climate could have been different in the past for certain time periods. Nevertheless, given the stability of the Holocene climate, we do not expect first-order changes of the signal and noise properties over time. However, we do expect a time-scale dependency of the climate signal with more variance associated with longer time scales (e.g., Pelletier, 1998). The signal-to-noise variance ratio and the climate representativity of firn cores will improve considerably on these scales.

### 4.3 Implications

Our noise level and implied climate representativity estimates underline the challenge of firn-core-based climate reconstructions ~~on seasonal to inter-annual time scales at seasonal to annual resolution~~ in low-accumulation regions. For our study site, we now discuss implications of our noise model concerning (1) the required measurement precision of water isotopes in the case of classical isotope thermometry, (2) the potential noise fraction in isotope signals of the EDML ice core and (3) the detectability of ~~an anthropogenic~~ a temperature trend.

Our estimates of the stratigraphic noise level are based on the upper one metre of firn. Due to the shortness of the data our results are limited by ~~our~~ insufficient knowledge of the vertical noise covariance structure for ~~time scales above annual resolution inter-annual and longer time scales~~ for which we now assume white-noise behaviour. The noise of isotopic data obtained from deeper parts of the firn column is affected by diffusion and densification. ~~The latter only is of importance for undated samples~~ Densification is only of importance when studying the isotopic time series in the depth domain as here, constantly sampled data will contain noise levels on varying time scales. We estimate the effect of diffusion and find that ~~for decadal time scales even at decadal resolution~~ below the firn-ice transition the ~~decadal~~ noise level at Kohnen station is ~~reduced by~~ only 5% smaller as compared to the undiffused case (Appendix B and Table 2) ~~compared to the undiffused case.~~

The noise of an isotopic signal includes the stratigraphic noise as well as noise caused by the measurement process. Since the stratigraphic noise is a function of the number of analysed cores, and measurement precision is often related to measurement time, obtaining the best signal is a trade-off between measurement precision and the amount of analysed samples.

~~For~~ At seasonal as well as ~~on inter-annual time scales~~ annual resolution, the measurement uncertainty of the trench data of  $\Delta\delta^{18}\text{O} = 0.09\%$   ~~$\sigma_{\text{CRDS}} = 0.09\%$~~  is much lower ( $\sim 4\text{--}10\%$ ) than the standard deviation of the stratigraphic noise (Table 2). This ratio is independent of the temporal resolution if a lower resolution is obtained by averaging annually

resolved data as both contributions decrease by the same amount in the averaging process, assuming independence between the samples. In such a case, priority should be given to measuring and averaging across multiple cores in order to reduce the (stratigraphic) noise levels instead of performing high-precision measurements on single cores. As an example, with the Cavity Ring-Down Spectrometers used for this work faster measurements are possible by reducing the number of repeated measurements per sample and applying a memory correction (van Geldern and Barth, 2012). We explicitly note that this possibility is limited to classical single-isotope ( $\delta^{18}\text{O}$ ) reconstructions as it can affect the data usability for diffusion- (Gkinis et al., 2014; van der Wel et al., 2015) or deuterium-excess-based (Vimeux et al., 2001) inferences.

If a lower temporal resolution is obtained by a coarser sampling of the cores, the measurement error to stratigraphic noise ratio will depend on the analysed resolution (Table 2). For a resolution corresponding to ten years, our measurement uncertainty might amount to up to 32% of the stratigraphic noise level, accounting for full diffusion. The noise level of single cores would become comparable to the measurement uncertainty for averages over  $\sim 104$  or  $\sim 735$  years (best- or worst-case scenario of annual noise level).

The deep EPICA DML ice core obtained in the vicinity of Kohnen station reflects the climate evolution in Antarctica over the last 150 000 years (EPICA community members, 2006). Oerter et al. (2004) studied a core section covering the last 6000 years ~~on~~ at decadal resolution. We find a  $\delta^{18}\text{O}$  variance for this section of  $\sim 0.57$  (‰)<sup>2</sup>. Using our diffusion-corrected stratigraphic noise variance estimates would imply that  $\sim 15$ – $100$ % (from best to worst case) of the observed decadal variance in the core might be noise (Table 2), masking the underlying climate variability. We note that this is only a rough estimate as the shortness of the trench data does not allow to fully assess the decadal noise covariance. In any case, averaging across multiple cores seems necessary in low-accumulation regions to reconstruct the climate variability of the last millennium. Alternatively, if only the magnitude of variability is of interest, the proxy variability has to be corrected for the noise contribution (e.g., Laepple and Huybers, 2013).

As a final example of applying our noise model, we test the influence of stratigraphic noise on the detectability of a linear trend at Kohnen station. This is motivated by the finding of Steig et al. (2009) that in the last 50 years the surface temperature over East Antarctica has warmed by about half a degree. While both the climate signal as well as the relationship between local temperature and isotopic signal are complex, we assess the detectability with a ~~toy~~-simplified model experiment. For this, we assume the climate signal to be a purely linear trend ( $0.5^{\circ}\text{C}/50\text{yr}$ ) and a linear isotope-to-temperature relationship ( $1\text{‰}\cdot\text{K}^{-1}$ ), further influenced only by post-depositional noise. In a Monte Carlo approach repeated  $10^5$  times, we create stacks from 50yr long  $\delta^{18}\text{O}$  profiles with post-depositional noise variances based on our two limiting cases (Table 2) ~~and~~, accounting for an average effect of diffusion on the annual noise levels over the 50 years (Appendix B) and assuming independent noise between the profiles (inter-profile spacings  $\gtrsim 10\text{m}$ ), and vary the number of averaged profiles. A trend in the stacked profile is successfully detected for an estimated trend that is significantly larger than zero ( $p = 0.05$ ); the estimated slope is defined to be correct when it lies in a range of 25% around the true slope. The probability for trend detection/slope determination is then the ratio of successful reconstructions to total number of realisations.

Drilling a single core, the probability to detect the trend or to reconstruct its slope is around ~~20%-25%~~ in the best-case and below 10% in the worst-case scenario (Fig. 9). To reliably ( $> 80\%$  of the cases) detect the warming over the East Antarctic Plateau, our results suggest that averaging across at least ~~~7-50~~ ~5-35 firn cores taken at spacings of 10m (Fig. 9) is needed, depending on the scenario for the annual noise variance. Inferring the right slope would need three times that number of cores. We note that more realistic assumptions about the isotopic signal (natural climate and atmospheric variability, varying isotope-temperature relationship, etc.) further complicate the trend detectability.

## 5 Conclusions

We presented extensive oxygen stable water isotope data derived from two snow trenches excavated at Kohnen station in the interior of Dronning Maud Land, Antarctica. The two-

dimensional approach allowed a thorough investigation of the representativity of single firn-core isotope profiles, as well as of the spatial structure of the signal and noise over spatial scales of up to 500 m and a time span of approximately five years.

The trench data confirm previous studies that single low-accumulation ( $\leq 100 \text{ mm w.eq. yr}^{-1}$ ) isotope profiles only show a weak coherent signal at least on sub-decadal time scales. We also demonstrate that the spatial average of a sufficient number of profiles provides representative isotopic signals, consistent with our finding that the local noise has a small horizontal decorrelation length ( $\sim 1.5 \text{ m}$ ). This also suggests stratigraphic noise to be the major contribution to the horizontal isotopic variability. A statistical noise model based on a first-order autoregressive process successfully explains the observed covariance structure and allows to reproduce the correlation statistics between the trenches.

Based on these results we infer appropriate sampling strategies. At our low-accumulation ( $64 \text{ mm w.eq. yr}^{-1}$ ) site an optimal spacing of about 10 m is necessary for a sufficient decorrelation of the stratigraphic noise. ~~For seasonal and annual resolution, we~~ We estimate the climate representativity of isotope profiles depending on the number of averaged firn cores and the inter-core spacing. Our estimates show that ~~for at~~ for at seasonal resolution five cores at this spacing are necessary to obtain representative ( $r > 0.9$ ) isotope signals; ~~on inter-annual time scales at annual resolution~~ on inter-annual time scales at annual resolution up to  $\sim 8$  times as many cores are needed. As climate variations are typically stronger on longer time scales than analysed here, the climate representativity of firn- and ice-core reconstructions for slower climate changes will likely be higher.

We present two ~~explicit~~ explicit examples of how the stratigraphic noise might hamper the quantitative interpretation of isotope in terms of climate variations at our study site. Our data suggest that at least 15% of the decadal variations seen in the EPICA DML ice core over the last 6000 years might be post-depositional noise, but the climate signal might also be masked by a much higher decadal noise level. A ~~toy simplified~~ toy simplified model experiment shows that the faithful reconstruction of the recent positive temperature trend observed over the East Antarctic Plateau likely requires averaging across at least ~~7-50~~ 7-50 ~~5-35~~ 5-35 firn cores. For single-

proxy ( $\delta^{18}\text{O}$ ) reconstructions this task could be rendered easier by the fact that the annual noise level is substantially larger than typical measurement uncertainties. Thus, monitoring the measurement error depending on sample throughput could allow fast measurements for the benefit of analysing many cores. Alternatively, using indirect methods based on diffusion (Gkinis et al., 2014; van der Wel et al., 2015) or gas isotope ratios (Kobashi et al., 2011) might circumvent the problem of stratigraphic noise.

Since the stratigraphic noise is related to irregular re-deposition and erosion of snow and the formation of surface dunes, it primarily depends on the local accumulation rate, besides further factors such as wind strength, temperature, seasonal timing of the precipitation and snow properties. Therefore, we expect that our representativity results improve (worsen) for regions with higher (lower) accumulation rates. In effect, our results are likely applicable for large parts of the East Antarctic Plateau, but similar studies in West Antarctica and Greenland – regions with considerably higher accumulation rates – are needed. In addition, studies with deeper trenches that cover a longer time period, complemented by spectral analyses of nearby firn cores, are necessary to enhance our knowledge of the vertical noise covariance structure. This is crucial to determine the climate representativity on longer time scales. Deeper trenches would also allow to link our representativity results to actual correlations with temperature time series derived from weather stations. The latter is part of ongoing work at Kohnen station.

## Appendix A: Derivation of noise model

### *Definitions*

We consider isotope profiles  $X_i(z)$  at equidistant spacings  $\Delta\ell$  where  $z$  is depth on absolute coordinates and  $i$  refers to the profile's horizontal position along a snow trench,  $\ell_i = \ell_0 + i \cdot \Delta\ell$ , with some arbitrary starting position  $\ell_0$  (Fig. A1). This and all subsequent nomenclature is summarised in Table A1.

We assume each  $X_i(z)$  as a sum of a common signal  $S(z)$  and a noise term  $w_i(z)$  independent of  $S$ ,

$$X_i(z) = S(z) + w_i(z). \quad (\text{A1})$$

The noise  $w_i(z)$  is modelled as an AR(1) process in the horizontal direction,

$$w_i(z) = aw_{i-1}(z) + \varepsilon_i(z), \quad (\text{A2})$$

where  $a$  is the autocorrelation parameter with  $0 \leq a \leq 1$  and  $\varepsilon_i(z)$  are independent random normal variables (white noise). We assume the same variance  $\text{var}(w)$  of the noise in both the horizontal and the vertical direction.

The mean of a set of  $N$  trench isotope profiles  $\overline{X}_{\{i\}}$  (profile stack) is defined by the indices  $\{i\} = \{i_1, i_1+i_2, i_1+i_2+i_3, \dots, i_1+i_2+\dots+i_N\}$ . This nomenclature of incremental steps simplifies the expressions obtained later.  $\overline{X}_{\{i\}}(z)$  is given by the signal  $S(z)$  and the mean of the noise terms,

$$\overline{X}_{\{i\}}(z) = S(z) + \frac{1}{N} (w_{i_1} + w_{i_1+i_2} + \dots + w_{i_1+i_2+\dots+i_N})(z). \quad (\text{A3})$$

The Pearson correlation of two single profiles  $X_i$  and  $X_{i+j}$  is

$$\text{corr}(X_i, X_{i+j}) = \frac{\text{cov}(X_i, X_{i+j})}{\sqrt{\text{var}(X_i)\text{var}(X_{i+j})}} = \frac{\text{var}(S) + \text{cov}(w_i, w_{i+j})}{\text{var}(S) + \text{var}(w)}, \quad (\text{A4})$$

using the independence of signal and noise and the stationarity of  $w$ .

The correlation of a profile stack  $\overline{X}_{\{i\}}$  and the signal is given by

$$\text{corr}(\overline{X}_{\{i\}}, S) = \frac{\text{cov}(\overline{X}_{\{i\}}, S)}{\sqrt{\text{var}(\overline{X}_{\{i\}})\text{var}(S)}} = \frac{\text{var}(S)}{\sqrt{\text{var}(\overline{X}_{\{i\}})\text{var}(S)}}. \quad (\text{A5})$$

Similarly, the correlation of two profile stacks with indices  $\{i\}$  and  $\{j\}$ , assuming independent noise between the sets, is obtained from

$$\text{corr}(\overline{X}_{\{i\}}, \overline{X}_{\{j\}}) = \frac{\text{cov}(\overline{X}_{\{i\}}, \overline{X}_{\{j\}})}{\sqrt{\text{var}(\overline{X}_{\{i\}})\text{var}(\overline{X}_{\{j\}})}} = \frac{\text{var}(S)}{\sqrt{\text{var}(\overline{X}_{\{i\}})\text{var}(\overline{X}_{\{j\}})}}. \quad (\text{A6})$$

### 5 Derivation of model correlations

To derive the explicit correlations (A4)–(A6) for the AR(1) noise model, we need expressions for the noise variance,  $\text{var}(w)$ , the noise covariance in horizontal direction,  $\text{cov}(w_i, w_{i+j})$ , and the variance of a profile stack,  $\text{var}(\overline{X}_{\{i\}})$ .

The former two are given by (Chatfield, 2004)

$$\text{var}(w) = \frac{\text{var}(\varepsilon)}{1 - a^2}, \quad (\text{A7})$$

$$\text{cov}(w_i, w_{i+j}) = \frac{\text{var}(\varepsilon)}{1 - a^2} a^j = \text{var}(w) a^j. \quad (\text{A8})$$

The index  $j$  can be expressed here by the distance  $d = \ell_{i+j} - \ell_i$  between the profiles  $X_i$  and  $X_{i+j}$  and the spacing of adjacent profiles  $\Delta\ell$  as  $j = d/\Delta\ell$ . Further, for an AR(1) process the lag one autocorrelation is given by  $a = \exp(-\Delta\ell/\lambda)$  with the decorrelation scale  $\lambda$ . It follows from (A8) that the horizontal noise covariance decreases exponentially with distance  $d$  as

$$\text{cov}(w_i, w_{i+j}) = \text{var}(w) \exp\left(-\frac{d}{\lambda}\right). \quad (\text{A9})$$

The variance of a profile stack  $\overline{X}_{\{i\}}$  is calculated according to

$$\begin{aligned} \text{var}(\overline{X}_{\{i\}}) &= \left\langle \overline{X}_{\{i\}}^2(z) \right\rangle - \left\langle \overline{X}_{\{i\}}(z) \right\rangle^2 \\ &= \text{var}(S) + \frac{1}{N^2} \left\langle (w_{i_1} + w_{i_1+i_2} + \dots + w_{i_1+i_2+\dots+i_N})^2(z) \right\rangle \end{aligned} \quad (\text{A10})$$

where  $\langle \cdot \rangle$  denotes the expected value. Using the multinomial identity  $(\xi_1 + \xi_2 + \dots + \xi_N)^2 = \sum_{i=1}^N \xi_i^2 + 2 \sum_{i=1}^{N-1} \sum_{j>i} \xi_i \xi_j$  yields

$$\begin{aligned} \text{var}(\bar{X}_{\{i\}}) = \text{var}(S) + \frac{1}{N^2} \left\{ N \text{var}(w) + \right. \\ 2 \left( \langle w_{i_1} w_{i_1+i_2} \rangle + \langle w_{i_1} w_{i_1+i_2+i_3} \rangle + \dots + \right. \\ \left. \langle w_{i_1} w_{i_1+i_2+i_3+\dots+i_N} \rangle + \langle w_{i_2} w_{i_2+i_3} \rangle + \dots + \right. \\ \left. \left. \langle w_{i_2} w_{i_2+i_3+\dots+i_N} \rangle + \dots + \langle w_{i_{N-1}} w_{i_{N-1}+i_N} \rangle \right) \right\}. \end{aligned} \quad (\text{A11})$$

By applying (A8) for the horizontal covariance of the noise we obtain

$$\begin{aligned} \text{var}(\bar{X}_{\{i\}}) = \text{var}(S) + \text{var}(w) \times \\ \frac{1}{N^2} \left\{ N + 2 \underbrace{(a^{i_2} + a^{i_2+i_3} + \dots + a^{i_2+\dots+i_N} + a^{i_3} + \dots + a^{i_3+\dots+i_N} + \dots + a^{i_N})}_{\sigma_{\{i\}}^{*2}} \right\} \end{aligned} \quad (\text{A12})$$

where we define  $\sigma_{\{i\}}^{*2}$  as the relative effective noise variance of the profile stack. In the limiting case of  $a = 0$  (zero autocorrelation)  $\sigma_{\{i\}}^{*2} = 1/N$ , in the limit of  $a = 1$  (perfect autocorrelation)  $\sigma_{\{i\}}^{*2} = 1$ . In general,  $\sigma_{\{i\}}^{*2}$  is a function of both  $N$  and the spacing of the profiles averaged (Fig. A2).

For final expressions of the correlation functions (A4)–(A6), we define the signal-to-noise variance ratio  $F := \frac{\text{var}(S)}{\text{var}(w)}$  and use (A9) and (A12) to obtain

$$\text{inter-profile corr.: } \text{corr}(X_i, X_{i+j}) = \frac{1}{1 + F^{-1}} \left\{ 1 + F^{-1} \exp\left(-\frac{d}{\lambda}\right) \right\}, \quad (\text{A13})$$

$$\text{stack-signal corr.: } \text{corr}(\bar{X}_{\{i\}}, S) = \frac{1}{\sqrt{1 + F^{-1}\sigma_{\{i\}}^{*2}}}, \quad (\text{A14})$$

$$\text{stack-stack corr.: } \text{corr}(\bar{X}_{\{i\}}, \bar{X}_{\{j\}}) = \frac{1}{\left\{ \left(1 + F^{-1}\sigma_{\{i\}}^{*2}\right) \left(1 + F^{-1}\sigma_{\{j\}}^{*2}\right) \right\}^{1/2}}. \quad (\text{A15})$$

### Estimation of parameters

5 To evaluate the correlation functions (A13)–(A15) we need estimates of the decorrelation length  $\lambda$  and of the time-scale dependent variance ratio  $F^{-1}$ .

For the trench data [on the seasonal time scale at seasonal resolution](#), we obtain a variance ratio of  $F^{-1} \simeq 1.1 \pm 0.1$  from the observed inter-profile correlations of T1 (Fig. 6) for profile spacings  $\geq 10$  m, and an estimate of the decorrelation length of  $\lambda \simeq 1.5$  m from the horizontal autocorrelation of the T1  $\delta^{18}\text{O}$  data. We validate the parameters by comparing the predicted (A15) and observed correlations between profile stacks derived from T1 and T2 (Fig. 7). This assumes independent noise between T1 and T2, a valid approximation given that the trench distance ( $\sim 500$  m) is much larger than  $\lambda$ . Relying on the assumption of equal noise variance in the horizontal and vertical direction, a second estimate of  $F^{-1} \sim 1.6$  can be obtained from the observed mean T1 down-core variance (identified with signal and noise) subtracted by the observed mean T1 horizontal variance (= noise).

Going from the original seasonal resolution of the trench data to an explicit [inter-annual time scale annual resolution](#), the short data sets only allow limited estimations. We thus make use of the following simple heuristic arguments. The annual signal variance is estimated from the mean annual  $\delta^{18}\text{O}$  time series of each trench neglecting the residual noise contributions and averaging both variance estimates to obtain  $\text{var}(S)_{\text{annual}} \simeq 0.68 (\%)^2$ . The annual noise variance,  $\text{var}(w)_{\text{annual}}$ , is calculated from the seasonal noise variance estimated by the mean horizontal T1 variance of  $\text{var}(w) \simeq 5.9 (\%)^2$ . Physically, we expect a vertical autocorrelation of the noise due to the underlying processes (stratigraphic noise, Fisher et al., 1985; Ekaykin et al., 2002; diffusion, [Johnsen et al., 2000](#)) which is also indicated by our data (Fig. 1b). However, due to the limited vertical trench data, the vertical

noise autocorrelation cannot be reliably estimated and we discuss two limiting cases: case I) the vertical noise is independent (white noise) and the seasonal noise variance therefore reduced by the number of samples included in the annual average ( $N \approx 7$ ), case II) the vertical noise shows complete inter-dependence on the sub-annual time scale and its variance is not reduced by taking annual means. The resulting inter-annual-annual variance ratios of noise over signal are

$$F_{\text{annual}}^{-1} = \frac{\text{var}(w)_{\text{annual}}}{\text{var}(S)_{\text{annual}}} \simeq \frac{1}{0.68} \times \begin{cases} 0.84, & \text{for case I,} \\ 5.9 & \text{for case II.} \end{cases} \quad (\text{A16})$$

For all longer time scales, we generally assume white-noise behaviour for the noise covariance.

## 10 Appendix B: Reduction of noise level by diffusion

The integral over the power spectrum  $P(f)$  of a time series  $X(t)$ , where  $f$  denotes frequency and  $t$  time, is equal to the total variance of  $X$  (Chatfield, 2004),

$$\text{var}(X) = 2 \int_0^{f_0} \underline{P(f) df} \int_{f_N}^f \underline{P(f) df}. \quad (\text{B1})$$

Here,  $f_0$  is the Nyquist frequency according to the sample resolution of  $X$ .

15 For a white noise, the power spectrum is a constant,  $P_0(f) = P_0 = \text{const}$ . Evaluation of Eq. (B1) then gives  $2f_N P_0$ .

In case of diffusion, the initial power spectrum  $P_0(f)$  is changed for a given diffusion length  $\sigma$  and local annual layer thickness  $\hat{b}$ , diffusion changes the initial power spectrum  $P_0(f)$  according to (van der Wel et al., 2015)

$$20 \quad P(f) = P_0(f) \underline{\exp\left(-2\pi\sigma\hat{b}^{-1}f\right)^2} \exp\left\{-\left(2\pi\sigma\hat{b}^{-1}f\right)^2\right\}, \quad (\text{B2})$$

where  $\dot{b}$  is introduced in order to work in the temporal domain, thus with frequency measured in  $\text{yr}^{-1}$ . For white noise, the initial power spectrum is a constant,  $P_0(f) = P_0 = \text{const}$ . In this case, the integral (B1) is straightforward to solve,

$$2P_0 \int_0^{f_0} \exp\left(-2\pi\sigma\dot{b}^{-1}f\right)^2 df = P_0\sqrt{\pi}/(2\pi\sigma\dot{b}^{-1}) \text{erf}(2\pi\sigma\dot{b}^{-1}f_0).$$

5 ~~We assume a layer thickness of ice of~~ yielding the noise variance at a given resolution  $f_N$  accounting for diffusion:

$$2P_0 \int_0^{f_N} \exp\left\{-\left(2\pi\sigma\dot{b}^{-1}f\right)^2\right\} df = P_0\sqrt{\pi}/(2\pi\sigma\dot{b}^{-1}) \text{erf}(2\pi\sigma\dot{b}^{-1}f_N). \quad (\text{B3})$$

To estimate how much diffusion has reduced the annual trench noise level at the firn-ice transition at decadal resolution ( $f_N = 0.05 \text{ yr}^{-1}$ ), we assume  $\dot{b} = 7 \text{ cm yr}^{-1}$  (equivalent to the present accumulation rate at Kohonen station of  $6.4 \text{ cm w.eq. yr}^{-1}$ ) to obtain an upper limit of the diffusion effect. Given an initial noise power  $P_0$  for annual resolution, and a constant diffusion length of  $\sigma = 8 \text{ cm}$  (Johnsen et al., 2000) and a Nyquist frequency of  $f_0 = 0.05 \text{ yr}^{-1}$  according to decadal resolution, evaluation of Evaluation of (B3) yields a reduction of the annual noise power of  $\sim 0.095[\text{yr}^{-1}]P_0$ , similar to the case. Comparing the diffused with the undiffused case shows that at decadal resolution, diffusion only has a relative effect of  $\sim 5\%$  on the reduction of undiffused white noise (reduction by a factor of 10). At our site, diffusion thus the annual noise level.

Thus, diffusion only has a minor effect influence on decadal and longer time scales at our study site. However, on shorter time scales it has to be accounted for. The annual noise levels given in Table 2 are therefore only valid for the uppermost part of the firn column where diffusion is almost negligible. In the deeper parts of the firn, they have been affected

by diffusion. In our simplified trend detection experiment, we assume over the first 9 m of firn ( $\sim$  the last 50 years) an average annual layer thickness of 15 cm and a mean diffusion length of  $\sigma \sim 5$  cm (Johnsen et al., 2000). Evaluation of Eq. (B3) then gives an average reduction of the annual noise level to  $\sim 73\%$  of the original value.

## 5 Appendix C: Data availability

The trench oxygen isotope data presented in this study are archived at the PANGAEA database (<http://www.pangaea.de>) under the DOI: (will follow). PANGAEA is hosted by the Alfred Wegener Institute Helmholtz Centre for Polar and Marine Research (AWI), Bremerhaven and the Center for Marine Environmental Sciences (MARUM), Bremen, Germany.

*Acknowledgements.* We thank all the scientists, technicians and the logistic support who worked at Kohnen station in the 2012/13 austral summer; especially Melanie Behrens, Tobias Binder, Andreas Frenzel, Katja Instenberg, Katharina Klein, Martin Schneebeli, [Holger Schubert](#), Jan Tell and Stefanie Weissbach, for assistance in creating the trench data set. We further thank the technicians of the isotope laboratories in Bremerhaven and Potsdam, especially York Schломann and Christoph Manthey. All plots and numerical calculations were carried out using the software R: A Language and Environment for Statistical Computing. This work was supported by the Initiative and Networking Fund of the Helmholtz Association Grant VG-NH900. [We thank the editor and two anonymous reviewers for their constructive comments that helped to improve the manuscript.](#)

## 20 References

- Birnbaum, G., Freitag, J., Brauner, R., König-Langlo, G., Schulz, E., Kipfstuhl, S., Oerter, H., Reijmer, C. H., Schlosser, E., Faria, S. H., Ries, H., Loose, B., Herber, A., Duda, M. G., Powers, J. G., Manning, K. W., and van den Broeke, M. R.: Strong-wind events and their influence on the formation of snow dunes: observations from Kohnen station, Dronning Maud Land, Antarctica, *J. Glaciol.*, 56, 891–902, 2010.
- Chatfield, C.: The analysis of time series: an introduction, 6th ed., Chapman & Hall/CRC, Boca Raton, ISBN: 1-58488-317-0, 2004.

- Cuffey, K. M. and Steig, E. J.: Isotopic diffusion in polar firn: implications for interpretation of seasonal climate parameters in ice-core records, with emphasis on central Greenland, *J. Glaciol.*, 44, 273–284, 1998.
- 5 Dansgaard, W., Johnsen, S. J., Clausen, H. B., Dahl-Jensen, D., Gundestrup, N. S., Hammer, C. U., Hvidberg, C. S., Steffensen, J. P., Sveinbjörnsdóttir, A. E., Jouzel, J., and Bond, G.: Evidence for general instability of past climate from a 250-kyr ice-core record, *Nature*, 364, 218–220, doi:10.1038/364218a0, 1993.
- 10 Ekaykin, A. A., Lipenkov, V. Y., Barkov, N. I., Petit, J. R., and Masson-Delmotte, V.: Spatial and temporal variability in isotope composition of recent snow in the vicinity of Vostok station, Antarctica: implications for ice-core record interpretation, *Ann. Glaciol.*, 35, 181–186, doi:10.3189/172756402781816726, 2002.
- EPICA community members: One-to-one coupling of glacial climate variability in Greenland and Antarctica, *Nature*, 444, 195–198, 2006.
- 15 Fisher, D. A., Koerner, R. M., Paterson, W. S. B., Dansgaard, W., Gundestrup, N., and Reeh, N.: Effect of wind scouring on climatic records from ice-core oxygen-isotope profiles, *Nature*, 301, 205–209, doi:10.1038/301205a0, 1983.
- Fisher, D. A., Reeh, N., and Clausen, H. B.: Stratigraphic noise in time series derived from ice cores, *Ann. Glaciol.*, 7, 76–83, 1985.
- 20 Gfeller, G., Fischer, H., Bigler, M., Schüpbach, S., Leuenberger, D., and Mini, O.: Representativeness and seasonality of major ion records derived from NEEM firn cores, *The Cryosphere*, 8, 1855–1870, doi:10.5194/tc-8-1855-2014, 2014.
- Gkinis, V., Simonsen, S. B., Buchardt, S. L., White, J. W. C., and Vinther, B. M.: Water isotope diffusion rates from the NorthGRIP ice core for the last 16,000 years – Glaciological and paleoclimatic implications, *Earth Planet. Sc. Lett.*, 405, 132–141, doi:10.1016/j.epsl.2014.08.022, 2014.
- 25 Graf, W., Oerter, H., Reinwarth, O., Stichler, W., Wilhelms, F., Miller, H., and Mulvaney, R.: Stable isotope records from Dronning Maud Land, Antarctica, *Ann. Glaciol.*, 35, 195–201, 2002.
- Helsen, M. M., van de Wal, R. S. W., van den Broeke, M. R., Masson-Delmotte, V., Meijer, H. A. J., Scheele, M. P., and Werner, M.: Modeling the isotopic composition of Antarctic snow using backward trajectories: simulation of snow pit records, *J. Geophys. Res.*, 111, D15109, doi:10.1029/2005JD006524, 2006.
- 30 Hoshina, Y., Fujita, K., Nakazawa, F., Iizuka, Y., Miyake, T., Hirabayashi, M., Kuramoto, T., Fujita, S., and Motoyama, H.: Effect of accumulation rate on water stable isotopes of near-surface snow in inland Antarctica, *J. Geophys. Res.*, 119, 274–283, doi:10.1002/2013JD020771, 2014.

- Huntingford, C., Jones, P. D., Livina, V. N., Lenton, T. M., and Cox, P. M.: No increase in global temperature variability despite changing regional patterns, *Nature*, 500, 327–330, doi:10.1038/nature12310, 2013.
- Johnsen, S. J.: Stable isotope homogenization of polar firn and ice, in: *Isotopes and Impurities in Snow and Ice*, no. 118 in *Proceedings of the Grenoble Symposium*, IAHS AISH Publ., Grenoble, France, 210–219, 1977.
- Johnsen, S. J., Clausen, H. B., Cuffey, K. M., Hoffmann, G., Schwander, J., and Creyts, T.: Diffusion of stable isotopes in polar firn and ice: the isotope effect in firn diffusion, in: *Physics of ice core records*, edited by: Hondoh, T., vol. 159, Hokkaido Univ. Press, Sapporo, Japan, 121–140, 2000.
- Jones, T. R., White, J. W. C., and Popp, T.: Siple Dome shallow ice cores: a study in coastal dome microclimatology, *Clim. Past*, 10, 1253–1267, doi:10.5194/cp-10-1253-2014, 2014.
- Karlöf, L., Winebrenner, D. P., and Percival, D. B.: How representative is a time series derived from a firn core? A study at a low-accumulation site on the Antarctic plateau, *J. Geophys. Res.*, 111, F04001, doi:10.1029/2006JF000552, 2006.
- Kobashi, T., Kawamura, K., Severinghaus, J. P., Barnola, J.-M., Nakaegawa, T., Vinther, B. M., Johnsen, S. J., and Box, J. E.: High variability of Greenland surface temperature over the past 4000 years estimated from trapped air in an ice core, *Geophys. Res. Lett.*, 38, L21501, doi:10.1029/2011GL049444, 2011.
- Laepfle, T. and Huybers, P.: Reconciling discrepancies between Uk37 and Mg/Ca reconstructions of Holocene marine temperature variability, *Earth Planet. Sc. Lett.*, 375, 418–429, doi:10.1016/j.epsl.2013.06.006, 2013.
- Laepfle, T. and Huybers, P.: Ocean surface temperature variability: large model–data differences at decadal and longer periods, *P. Natl. Acad. Sci. USA*, 111, 16682–16687, doi:10.1073/pnas.1412077111, 2014.
- Laepfle, T., Werner, M., and Lohmann, G.: Synchronicity of Antarctic temperatures and local solar insolation on orbital timescales, *Nature*, 471, 91–94, doi:10.1038/nature09825, 2011.
- Legrand, M. and Mayewski, P.: Glaciochemistry of polar ice cores: a review, *Rev. Geophys.*, 35, 219–243, doi:10.1029/96RG03527, 1997.
- McMorrow, A. J., Curran, M. A. J., Van Ommen, T. D., Morgan, V. I., and Allison, I.: Features of meteorological events preserved in a high-resolution Law Dome (East Antarctica) snow pit, *Ann. Glaciol.*, 35, 463–470, doi:10.3189/172756402781816780, 2002.
- Mosley-Thompson, E., McConnell, J. R., Bales, R. C., Li, Z., Lin, P.-N., Steffen, K., Thompson, L. G., Edwards, R., and Bathke, D.: Local to regional-scale variability of annual net accu-

- mulation on the Greenland ice sheet from PARCA cores, *J. Geophys. Res.*, 106, 33839–33851, doi:10.1029/2001JD900067, 2001.
- NEEM community members: Eemian interglacial reconstructed from a Greenland folded ice core, *Nature*, 493, 489–494, doi:10.1038/nature11789, 2013.
- 5 Neumann, T. A. and Waddington, E. D.: Effects of firn ventilation on isotopic exchange, *J. Glaciol.*, 50, 183–194, 2004.
- [Oerter, H., Wilhelms, F., Jung-Rothenhausler, F., Goktas, F., Miller, H., Graf, W., and Sommer, S.: Accumulation rates in Dronning Maud Land, Antarctica, as revealed by dielectric-profiling measurements of shallow firn cores, \*Ann. Glaciol.\*, 30, 27–34, 2000.](#)
- 10 Oerter, H., Graf, W., Meyer, H., and Wilhelms, F.: The EPICA ice core from Dronning Maud Land: first results from stable-isotope measurements, *Ann. Glaciol.*, 39, 307–312, 2004.
- Pelletier, J. D.: The power spectral density of atmospheric temperature from time scales of  $10^{-2}$  to  $10^6$  yr, *Earth Planet. Sc. Lett.*, 158, 157–164, 1998.
- Persson, A., Langen, P. L., Ditlevsen, P., and Vinther, B. M.: The influence of precipitation weighting on interannual variability of stable water isotopes in Greenland, *J. Geophys. Res.*, 116, D20120, doi:10.1029/2010JD015517, 2011.
- 15 Petit, J. R., Jouzel, J., Raynaud, D., Barkov, N. I., Barnola, J.-M., Basile, I., Bender, M., Chappellaz, J., Davis, M., Delaygue, G., Delmotte, M., Kotlyakov, V. M., Legrand, M., Lipenkov, V. Y., Lorius, C., Pépin, L., Ritz, C., Saltzman, E., and Stievenard, M.: Climate and atmospheric history of the past 420,000 years from the Vostok ice core, Antarctica, *Nature*, 399, 429–436, doi:10.1038/20859, 1999.
- 20 Raynaud, D., Jouzel, J., Barnola, J.-M., Chappellaz, J., Delmas, R. J., and Lorius, C.: The ice record of greenhouse gases, *Science*, 259, 926–934, doi:10.1126/science.259.5097.926, 1993.
- Rehfeld, K., Marwan, N., Heitzig, J., and Kurths, J.: Comparison of correlation analysis techniques for irregularly sampled time series, *Nonlin. Processes Geophys.*, 18, 389–404, doi:10.5194/npg-18-389-2011, 2011.
- 25 Sime, L. C., Marshall, G. J., Mulvaney, R., and Thomas, E. R.: Interpreting temperature information from ice cores along the Antarctic Peninsula: ERA40 analysis, *Geophys. Res. Lett.*, 36, L18801, doi:10.1029/2009GL038982, 2009.
- 30 Sime, L. C., Lang, N., Thomas, E. R., Benton, A. K., and Mulvaney, R.: On high-resolution sampling of short ice cores: dating and temperature information recovery from Antarctic Peninsula virtual cores, *J. Geophys. Res.*, 116, D20117, doi:10.1029/2011JD015894, 2011.

- Sommer, S., Appenzeller, C., Röthlisberger, R., Hutterli, M. A., Stauffer, B., Wagenbach, D., Oerter, H., Wilhelms, F., Miller, H., and Mulvaney, R.: Glacio-chemical study spanning the past 2 kyr on three ice cores from Dronning Maud Land, Antarctica: 1. Annually resolved accumulation rates, *J. Geophys. Res.*, 105, 29411–29421, doi:10.1029/2000JD900449, 2000a.
- 5 Sommer, S., Wagenbach, D., Mulvaney, R., and Fischer, H.: Glacio-chemical study spanning the past 2 kyr on three ice cores from Dronning Maud Land, Antarctica: 2. Seasonally resolved chemical records, *J. Geophys. Res.*, 105, 29423–29433, 2000b.
- Steen-Larsen, H. C., Masson-Delmotte, V., Hirabayashi, M., Winkler, R., Satow, K., Prié, F., Bayou, N., Brun, E., Cuffey, K. M., Dahl-Jensen, D., Dumont, M., Guillevic, M., Kipfstuhl, S., Landais, A., Popp, T., Risi, C., Steffen, K., Stenni, B., and Sveinbjörnsdóttir, A. E.: What controls the isotopic composition of Greenland surface snow?, *Clim. Past*, 10, 377–392, doi:10.5194/cp-10-377-2014, 2014.
- Steig, E. J., Schneider, D. P., Rutherford, S. D., Mann, M. E., Comiso, J. C., and Shindell, D. T.: Warming of the Antarctic ice-sheet surface since the 1957 International Geophysical Year, *Nature*, 15 457, 459–462, doi:10.1038/nature07669, 2009.
- Town, M. S., Warren, S. G., von Walden, P., and Waddington, E. D.: Effect of atmospheric water vapor on modification of stable isotopes in near-surface snow on ice sheets, *J. Geophys. Res.*, 113, D24303, doi:10.1029/2008JD009852, 2008.
- van der Wel, G., Fischer, H., Oerter, H., Meyer, H., and Meijer, H. A. J.: Estimation and calibration of the water isotope differential diffusion length in ice core records, *The Cryosphere*, 9, 1601–1616, doi:10.5194/tc-9-1601-2015, 2015.
- van Geldern, R. and Barth, J. A. C.: Optimization of instrument setup and post-run corrections for oxygen and hydrogen stable isotope measurements of water by isotope ratio infrared spectroscopy (IRIS), *Limnol. Oceanogr.-Meth.*, 10, 1024–1036, doi:10.4319/lom.2012.10.1024, 2012.
- 25 Vimeux, F., Masson, V., Delaygue, G., Jouzel, J., Petit, J. R., and Stievenard, M.: A 420,000 year deuterium excess record from East Antarctica: Information on past changes in the origin of precipitation at Vostok, *J. Geophys. Res.*, 106, 31863–31873, doi:10.1029/2001JD900076, 2001.
- Waddington, E. D., Steig, E. J., and Neumann, T. A.: Using characteristic times to assess whether stable isotopes in polar snow can be reversibly deposited, *Ann. Glaciol.*, 35, 118–124, 2002.
- 30 Whillans, I. M. and Grootes, P. M.: Isotopic diffusion in cold snow and firn, *J. Geophys. Res.*, 90, 3910–3918, doi:10.1029/JD090iD02p03910, 1985.

Wigley, T. M. L., Briffa, K. R., and Jones, P. D.: On the average value of correlated time series, with applications in dendroclimatology and hydrometeorology, *J. Clim. Appl. Meteorol.*, 23, 201–213, doi:10.1175/1520-0450(1984)023<0201:OTAVOC>2.0.CO;2, 1984.

**Table 1.** Variance levels of the two trenches: The horizontal variance is the mean variance of all depth layers on absolute coordinates, the down-core variance is the mean vertical variance of all respective trench profiles. The seasonal as well as the inter-annual-annual variance levels denote the variances of the respective mean seasonal and inter-annual-annual  $\delta^{18}\text{O}$  time series of the two trenches (Fig. 5). All numbers are in units of  $(\%)^2$ .

trench	horizontal $\sigma_h^2$	down-core $\sigma_v^2$	seasonal $\bar{\sigma}_v^2$	<u>inter-annual-annual</u> $\bar{\sigma}_a^2$
T1	5.9	9.5	5.1	1.15
T2	5.3	7.3	3.3	0.21

**Table 2.** Noise variance and standard deviation (SD) of the trench data together with the ratio of measurement uncertainty ( $\Delta\delta^{18}\text{O} = 0.09\%$ ,  $\sigma_{\text{CRDS}} = 0.09\%$ ) and respective noise SD, given for different time scales resolutions and for the two limiting cases of the annual noise variance. The decadal noise level estimates are calculated from the annual noise variances accounting for full forward diffusion.

<u>time scale</u> <u>resolution</u>	variance in $(\%)^2$	SD in %	$\Delta\delta^{18}\text{O}/\text{SD}$ $\sigma_{\text{CRDS}}/\text{SD}$
seasonal	5.9	2.43	4 %
annual: case I	0.84	0.92	10 %
annual: case II	5.9	2.43	4 %
<u>+10yr-avg.</u> <u>decadal</u> : case I	0.08	0.28	32 %
<u>+10yr-avg.</u> <u>decadal</u> : case II	0.56	0.75	12 %

**Table A1.** Summary of the nomenclature used for the statistical noise model.

symbol	description
$z$	absolute depth below mean snow height
$X_i$	trench isotope profile at position $\ell_i$
$\Delta\ell$	spacing of adjacent profiles
$S$	climate signal contained in $X_i$
$w_i$	noise contained in $X_i$
$\varepsilon_i$	white noise component of $w_i$
$\overline{X}_{\{i\}}$	profile stack
$a$	autocorrelation parameter; $a = \exp(-\Delta\ell/\lambda)$
$\lambda$	horizontal noise decorrelation length
$d$	inter-profile distance
$N$	number of profiles
$\sigma_{\{i\}}^{*2}$	relative effective noise variance of stack $\overline{X}_{\{i\}}$
$F$	signal-to-noise variance ratio

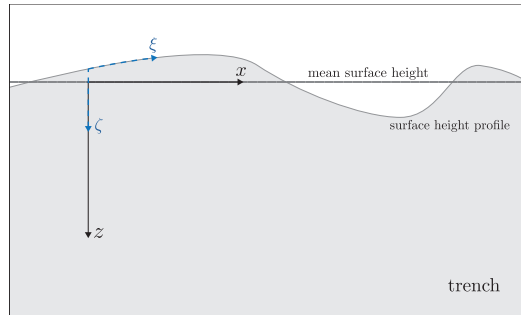


**Figure 1.** Coordinate systems used for the analysis of the trench isotope data: (1) a curvilinear coordinate system  $(\xi, \zeta)$  (blue dashed lines, surface coordinates) with horizontal axis **tangential to along** the surface height profile and vertical axis denoting the depth below the local surface; (2) a Cartesian system  $(x, z)$  (black lines, absolute coordinates) defined by the mean surface height.

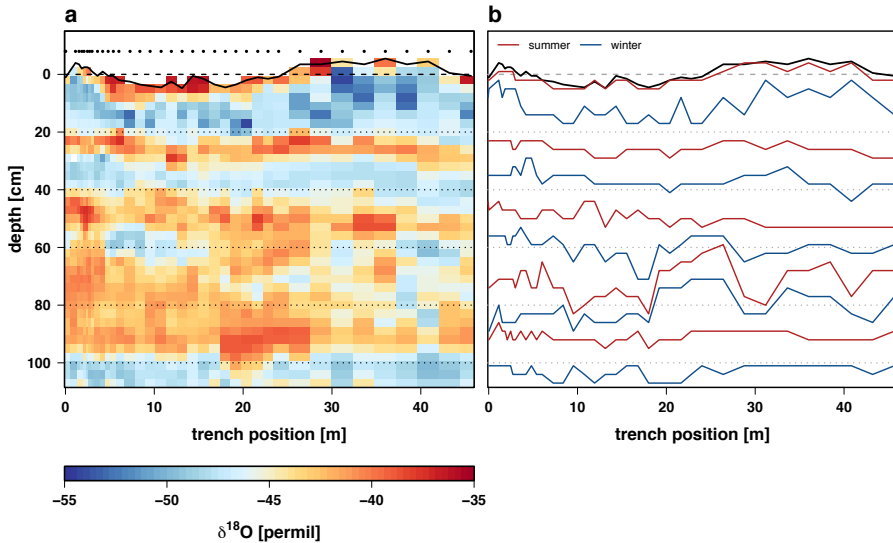


**Figure 2. a:** The two-dimensional  $\delta^{18}\text{O}$  data set of trench T1 displayed on absolute coordinates. The solid black line shows the surface height profile, the long-dashed black line the mean surface height. Sampling positions are marked by the black dots above. White gaps indicate missing data. **b:** The stratigraphy of trench T1 expressed as the seasonal layer profiles tracking the local  $\delta^{18}\text{O}$  extrema as explained in the text.

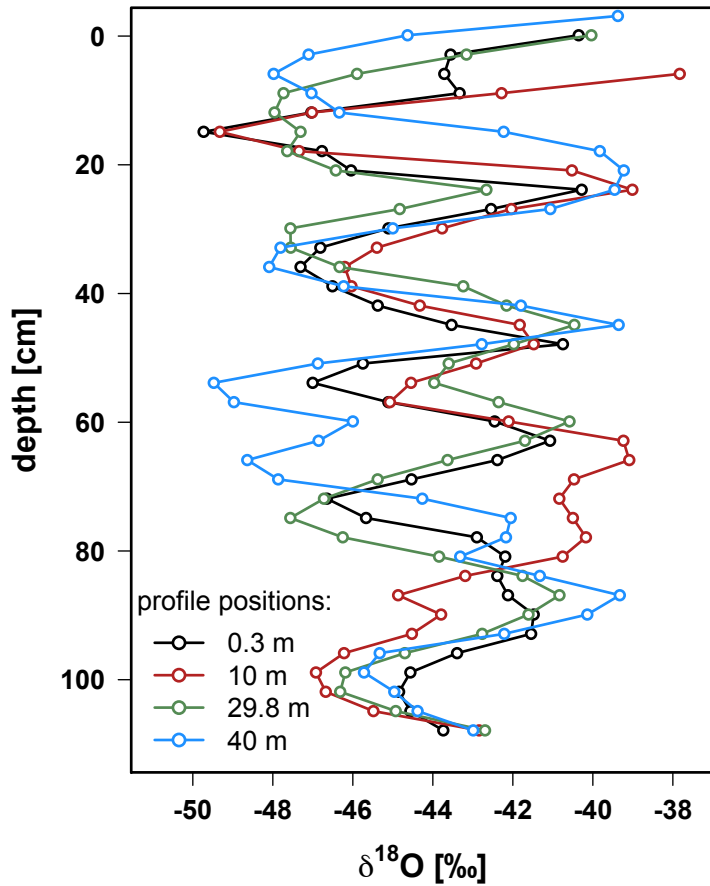


**Figure 3.** The four  $\delta^{18}\text{O}$  profiles obtained from trench T2 displayed on absolute coordinates.

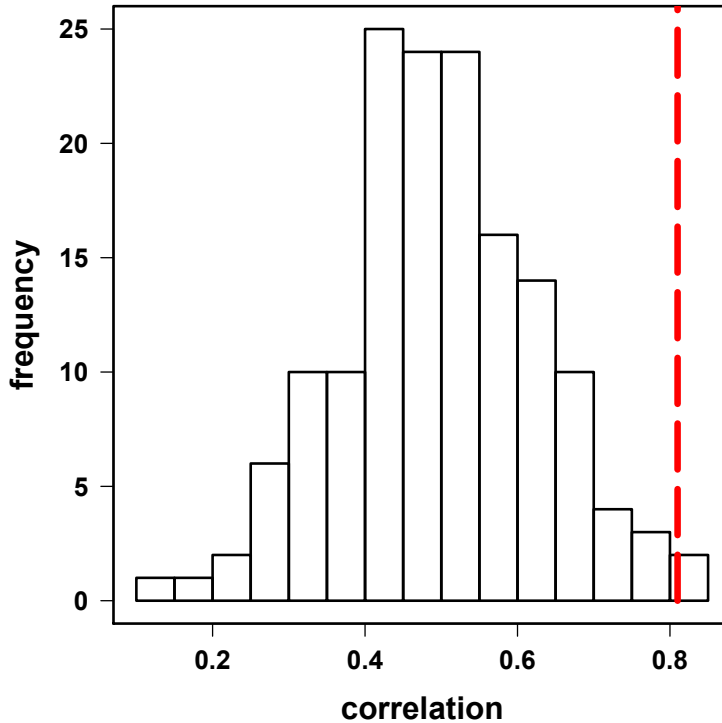


**Figure 4.** Histogram of all possible pairwise correlations ( $N = 152$ ) between single profiles of trench T1 and single profiles of trench T2. Displayed are the maximum correlations allowing vertical shifts of the T2 profiles of up to  $\pm 12$ cm. Shown in red is the correlation between the mean profiles of T1 and T2 (Fig. 5).

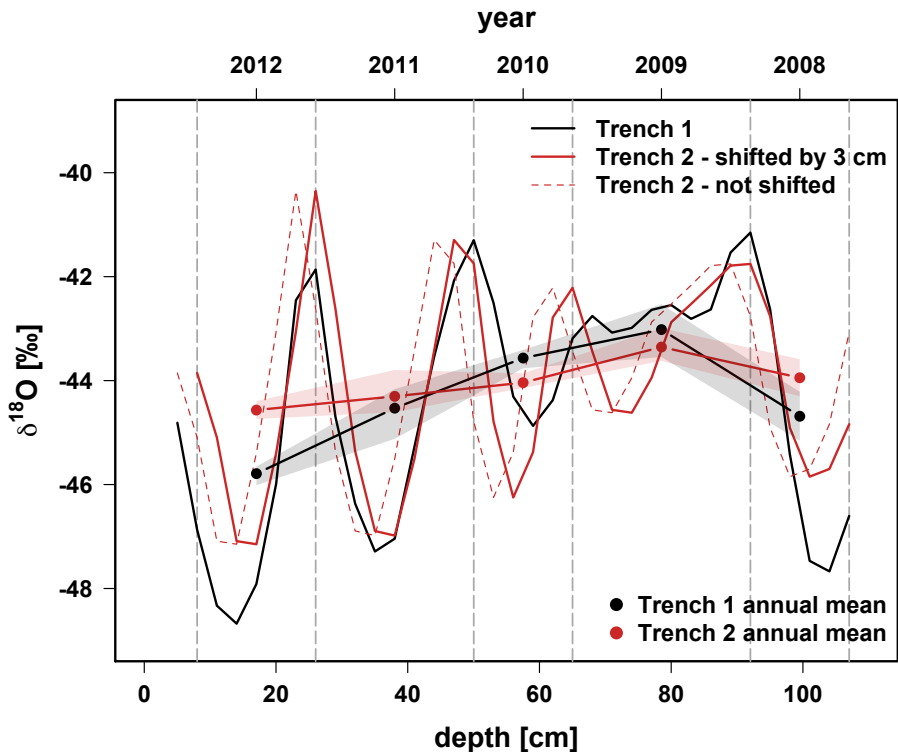


**Figure 5.** Comparison of the mean  $\delta^{18}\text{O}$  profiles (lines: seasonal, points: annual mean) from T1 (black) and T2 (red). To maximise the seasonal correlation ( $r_{T1,T2} = 0.81$ ), trench T2 was shifted by +3cm. For the first three depth bins, the number of existing observations varies on absolute coordinates between the trench profiles. To obtain non-biased seasonal mean profiles only the depth range covered by all profiles is used. Shadings represent the range of the approximate annual-mean profiles due to different binning definitions. Note that their first and last value are biased since the trench data are incomplete here. Vertical dashed grey lines mark the six local maxima of the average of both seasonal mean profiles.

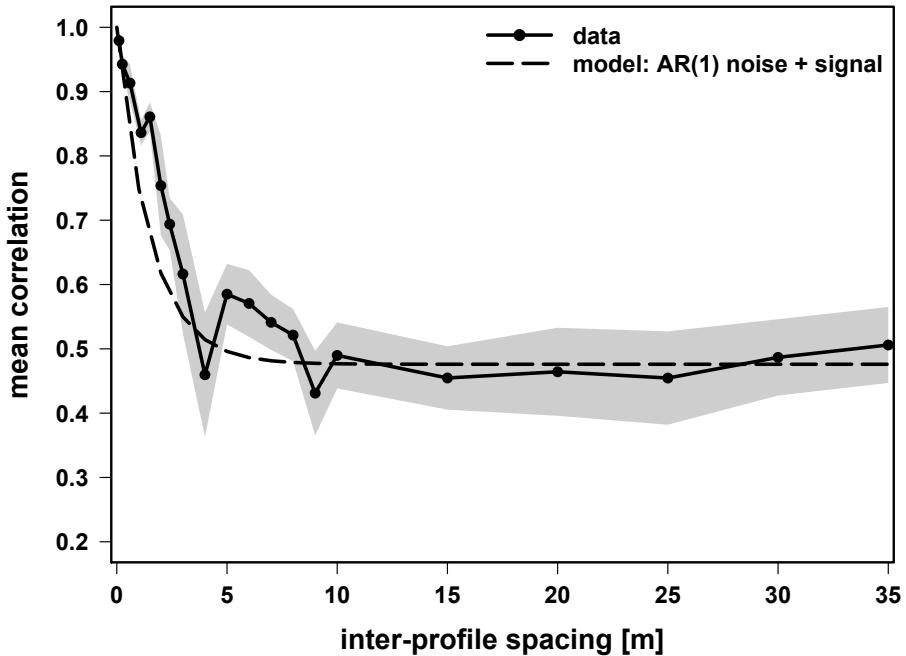


**Figure 6.** Observed and modelled inter-profile correlation as a function of profile spacing for T1. Observations for a given spacing are the mean across all possible profile pairs. Shadings denote the standard error of the mean assuming maximum degrees of freedom (DOF) of  $N = 12$  (estimated from the effective DOF of the horizontal trench data accounting for autocorrelation).

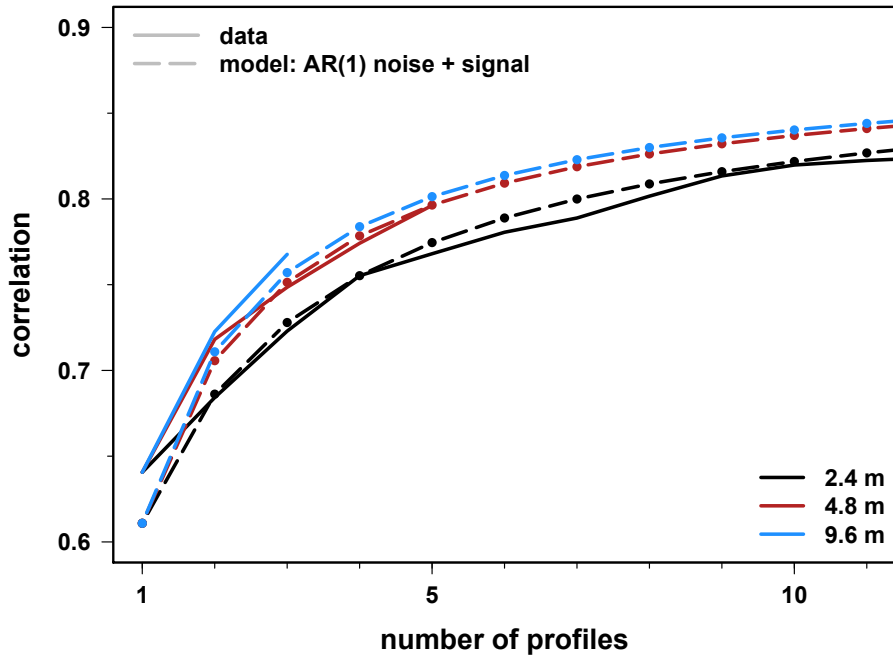


**Figure 7.** Observed and modelled correlations between T1 profile stacks and the mean of all T2 profiles depending on the number of profiles in the T1 stack for three selected inter-profile spacings. Observed results for given spacing and number of profiles are the mean across the correlations obtained for all possible unique stacks and only calculated when at least 15 stacks are available.

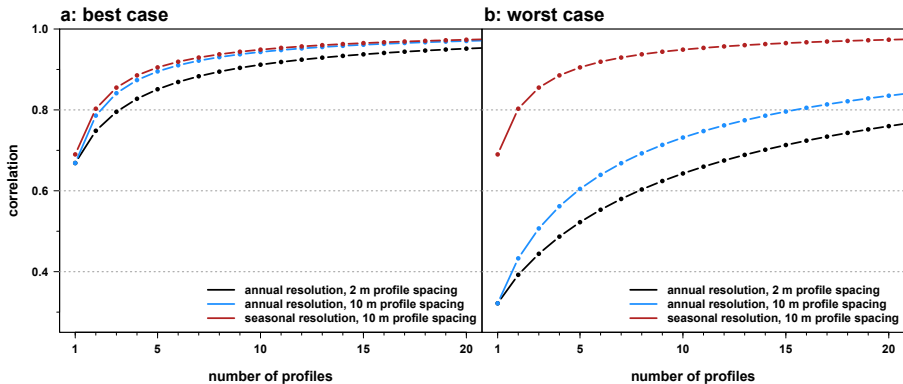


**Figure 8.** Representativity of a  $\delta^{18}\text{O}$  firn profile stack expressed as the correlation with a hypothetical climate signal depending on the number of profiles averaged and their inter-profile spacing. For **the inter-annual time scale annual resolution**, the two limiting cases discussed in the text are displayed (**a**: best-case scenario, **b**: worst-case scenario), each for 2 m (black) as well as 10 m (blue) inter-profile spacing. As a reference, in each case the seasonal representativity is shown in red for 10 m inter-profile spacing.

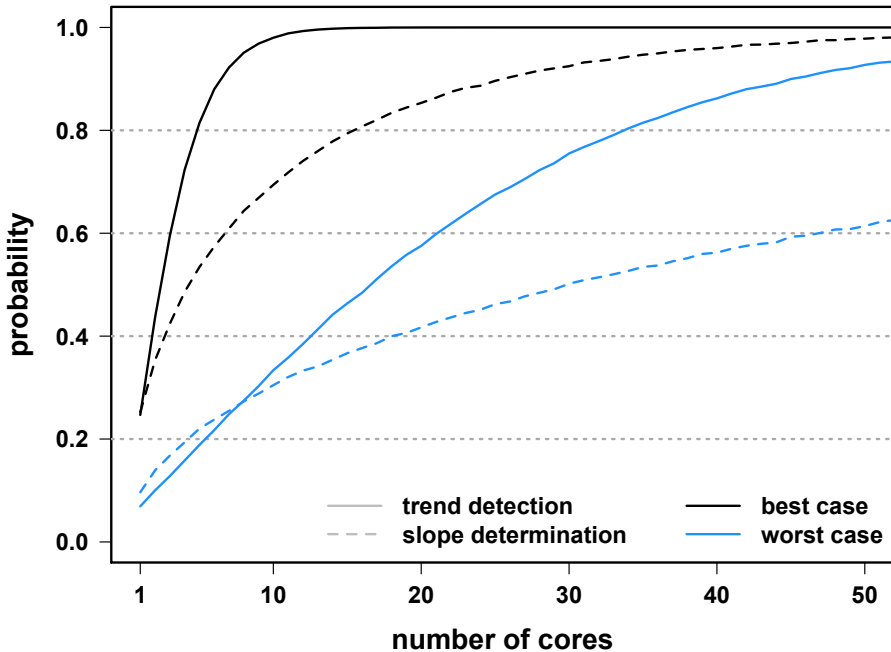


**Figure 9.** Probability of detecting a linear temperature trend of  $0.5^{\circ}\text{C}/50\text{ yr}$  ( $p = 0.05$ ) (solid lines) and of determining the strength of the trend with an accuracy of 25% (dashed lines) as a function of the number of firm cores averaged and for the two scenarios of the annual noise variance discussed in the text (black: best case, blue: worst case).

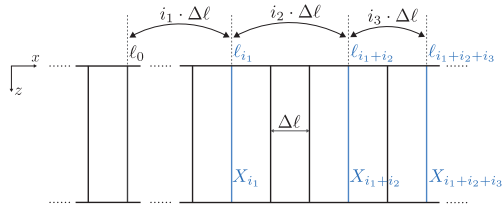


**Figure A1.** Sketch of a snow trench used for the derivation of the statistical noise model. Vertical isotope profiles  $X_i$  are spaced at constant intervals of  $\Delta\ell$  at locations  $\ell_i = \ell_0 + i\Delta\ell$ . The horizontal distance  $d$  between two profiles  $X_{i_1}$  and  $X_{i_1+i_2}$  is defined by the incremental index  $i_2$ ,  $d = i_2\Delta\ell$ .

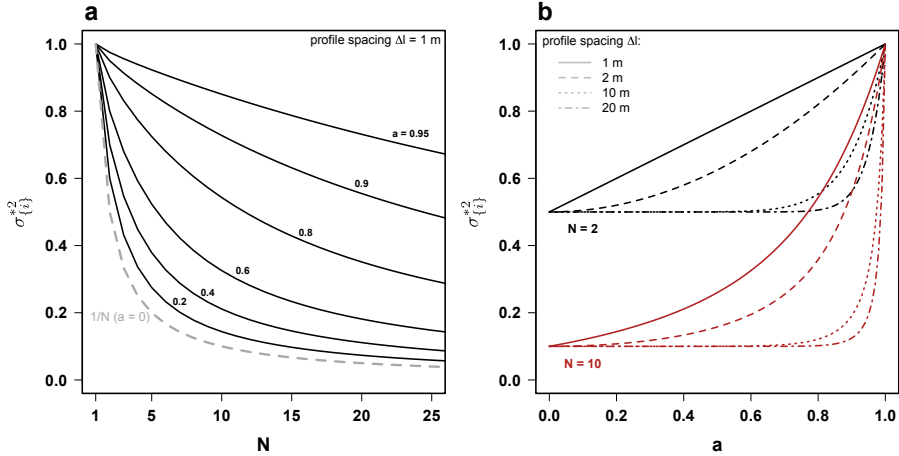


**Figure A2. a:** Relative effective noise variance  $\sigma_{\{i\}}^{*2}$  of a profile stack  $\bar{X}_{\{i\}}$  as a function of the number of profiles averaged for a profile spacing of  $\Delta l = 1$  m and for different values of the autocorrelation parameter  $a$ . The limiting case of white noise ( $a = 0$ ) is indicated by a dashed line. **b:**  $\sigma_{\{i\}}^{*2}$  as a function of the autocorrelation parameter  $a$  for different numbers of averaged profiles and profile spacings.